TU Delft

Delft University of Technology

An integrated approach to subtractive solar envelopes based on attribute information from point cloud data

Alkadri, Miktha; De Luca, Francesco; Turrin, Michela; Sariyildiz, Sevil

DOI
10.1016/j.rser.2020.109742

Publication date
2020

Document Version
Final published version

Published in
Renewable & Sustainable Energy Reviews

Citation (APA)
Alkadri, M., De Luca, F., Turrin, M., & Sariyildiz, S. (2020). An integrated approach to subtractive solar envelopes based on attribute information from point cloud data. *Renewable & Sustainable Energy Reviews*, *123*, Article 109742. https://doi.org/10.1016/j.rser.2020.109742

Important note
To cite this publication, please use the final published version (if applicable).
Please check the document version above.

Copyright
Other than for strictly personal use, it is not permitted to download, forward or distribute the text or part of it, without the consent of the author(s) and/or copyright holder(s), unless the work is under an open content license such as Creative Commons.

Takedown policy
Please contact us and provide details if you believe this document breaches copyrights.
We will remove access to the work immediately and investigate your claim.

This work is downloaded from Delft University of Technology.
For technical reasons the number of authors shown on this cover page is limited to a maximum of 10.

Renewable and Sustainable Energy Reviews 123 (2020) 109742

Contents lists available at ScienceDirect

Renewable and Sustainable Energy Reviews

journal homepage: http://www.elsevier.com/locate/rser

An integrated approach to subtractive solar envelopes based on attribute information from point cloud data

Miktha Farid Alkadri [a,*], Francesco De Luca [b], Michela Turrin [a], Sevil Sariyildiz [a]

[a] Chair of Design Informatics, Faculty of Architecture and the Built Environment, Delft University of Technology, Julianalaan 134, 2628BL, Delft, the Netherlands
[b] Department of Civil Engineering and Architecture, Tallinn University of Technology, Ehitajate tee 5, 19086, Tallinn, Estonia

ARTICLE INFO

Keywords:
Subtractive solar envelopes
Point cloud data
Passive design strategy
Material properties
Computational design method

ABSTRACT

As a passive design strategy, solar envelopes play a significant role in determining building mass based on desirable sun access during a predefined period. Nowadays, advancements in the area of computational tools permit designers to develop new methods for establishing solar envelopes. However, current approaches lack an understanding of the existing environment's site characteristics, especially when dealing with geometrical information about the surrounding context. Consequently, this aspect affects the contextual analysis process during the generation of solar envelopes because of insufficient information for the relevant input of simulation modelling. With the support of geometric and radiometric properties stored in point cloud data, such as position (XYZ), colour (RGB), and reflection intensity (I), this study has proposed novel subtractive solar envelopes that specifically consider the surface properties of the existing environment. Through a subtractive mechanism, the proposed method caters to several computational frameworks such as dataset pre-processing that aims to correct erroneous measurement during scanning. In alignment with that, the proposed building's visible sun vectors, optimal normal values, and 3D polyhedra are generated for the hit-or-miss analysis of subtractive solar envelopes. Furthermore, environmental assessments consisting of insolation and glare analysis are performed on the solar envelopes' final geometry. These performance assessments aim to investigate the potential and impact of the generated solar envelopes as it pertains to the existing buildings. Ultimately, this study supports architects not only in producing a new generation of subtractive solar envelopes based on real contextual settings but also in comprehensively understanding the microclimate condition of design context.

1. Introduction

Interrelations between new buildings and existing context play a significant role in achieving appropriate solar access in the built environment [1]. It is necessary to understand these relations during the early design phase in order to maximise proper daylight within the design process and address microclimatic conditions for a sustainable approach. The significance of this approach has been mentioned explicitly in The United Nations Framework Convention on Climate Change, specifically in Article 4, which addresses the improvement of environmental quality as a response to climate change [2]. In the built environment, it is crucial to avert any potential unforeseeable failures once a new building has been built. These failures may very well consist of unexpected microclimatic impacts created by a building and imposed on the local context (and vice versa). For example, the building at 20 Fenchurch Street in London, EC3M 8AQ, United Kingdom (2014) has reflected an extreme amount of sun glare into its surroundings because of its glazed, curved south façade. Multiple reports of severe effects have confirmed this issue; such reports include incidents such as a melted car, a heatwave around the building that exceeded 70° Celsius, and the high cost of finally fixing the design flaw of the façade [3]. On the other hand, a new UCL student housing building, which is located at 465 Caledonian Road, North London, N7 9GU, United Kingdom, perfectly exemplifies a poor relationship between a new building and the existing context. As a result of the student housing building's poor suitability to its environment, over 175 rooms receive an insufficient amount of direct sun access because the building's windows are obstructed by a historic 19th century façade. These cases clearly show a lack of design integration between new buildings and existing contexts. Given that architects have a responsibility to ensure a reciprocal relationship, it is necessary to start

* Corresponding author. Delfgauwseweg 165, 2628 EM, Delft, the Netherlands.
E-mail addresses: mikthafarid@gmail.com, M.F.Alkadri@tudelft.nl (M.F. Alkadri), francesco.deluca@taltech.ee (F. De Luca), M.Turrin@tudelft.nl (M. Turrin), I.S.Sariyildiz@tudelft.nl (S. Sariyildiz).

https://doi.org/10.1016/j.rser.2020.109742
Received 4 September 2019; Received in revised form 25 December 2019; Accepted 30 January 2020
1364-0321/© 2020 The Authors. Published by Elsevier Ltd. This is an open access article under the CC BY license (http://creativecommons.org/licenses/by/4.0/).

at an appropriate point during the preliminary design process, especially when dealing with solar access performance.

The concept of solar envelopes presents a contextual design approach that has great relevance for addressing the aforementioned issues. Designers can use solar envelopes to define solar access between a proposed building and its surrounding context. Initially introduced by Knowles [4,5], this concept consists of an imaginary mass that allows adjacent buildings the required amount of direct sun access. Since then, several variations of solar envelopes have been proposed [6,7]. However, the existing method has several gaps in contextual analysis: for example, cut-off times that merely focus on a fixed period, resulting in surrounding facades hardly receiving the same quality of direct sun access due to different site orientations and obstructions. In addition, solar envelopes' geometric properties rely heavily on the Z-axis of neighbouring facades' shadow fences, resulting in the limiting of the design configuration of solar envelopes during the simulation process. Subtractive solar envelopes were developed in response to these issues [8]; these are constructed on the basis of specific quantities of direct sunlight hours as obtained from the surrounding windows of existing building's facades. The subtractive approach also allows for the generation of a larger volumetric size of solar envelopes, which is useful for high-rise buildings in fragmented urban environments [9].

Nevertheless, the integration of subtractive mechanisms into design practices needs to comply with several critical aspects such as sun visibility and ray tracing analysis. *First*, the selection of visible sun data aims to identify the number of sunlight hours that are being blocked (or not) by adjacent buildings. The issue that matters most is that the resulting areas that are identified as having blocked sun are only dependent on the building-oriented context. Consequently, these areas are assumed to be located on a clear plot, which is due to an absence of characteristics and relevant site properties (e.g. vegetation) [10,11]. *Second*, the use of centroid points on surrounding windows during ray tracing analysis primarily counts on a sample of surrounding windows, which is limited to representing the area of neighbouring facades. Indeed, these issues may affect environmental performance calculations during solar envelope simulation, especially in relation to solar radiation analysis between planned and existing buildings.

In order to compensate for missing features within the current workflow of subtractive solar envelopes, this study has employed the technological advancement of 3D laser scanning that includes point cloud data. Its potential application may support several contributions, which are as follows:

- The geometric information offered by point clouds may fill the gaps in sun visibility analysis since it can significantly cover buildings and their surrounding objects. This section specifically provides information about the surfaces that are the most and the least exposed to the sun, and the existing facades. Accordingly, the resulting areas with blocked sun (indicated as the surfaces that are the least exposed to the sun) can be eliminated because those areas are shaded by the surroundings (e.g. buildings and vegetation).
- Ray tracing simulation can be performed on each point that is found in the point cloud dataset, which can be used as an alternative to a limited sample of the surrounding windows. This allows for the identification of any obstructed areas within the 3D polyhedra (a proposed building). Voxels that consist of 0 obstructions can be transformed into solar envelopes while voxels with values above 0 need to be disregarded due to an obstruction of surrounding buildings' direct sun access.
- Radiometric point cloud information (RGB colour and reflection intensity) can be utilised to detect material behaviours in existing environments. This is specifically done by investigating both optical (reflectivity and translucency) and thermal properties (albedo and emissivity) calculated from a point cloud of the contextual dataset. Thus, material performance analysis between a planned and an existing building can be performed. This is achieved by projecting the ray tracing of the surrounding buildings to the final geometry of solar envelopes.

This study has primarily focused on the development of the computational workflow of subtractive solar envelopes based on attribute information from point cloud data. Two aspects of the workflow have been presented in previous papers. *First*, a previous paper presented the basic mechanism of subtractive solar envelopes [9]. This work focused on generating and subtracting a proposed buildings' 3D matrix based on a sunlight hours analysis that came from surrounding buildings' windows. This idea has stimulated the further exploration of methods for establishing computational solar envelopes based on point cloud data. *Second*, another previous paper has presented on the correction of the preliminary dataset and the calculation of material properties based on attribute information stored in a point cloud [12]. The dataset correction contributes to the extraction of the dataset's optimal normal values while material properties become an input parameter for performing glare analysis on the final geometry of solar envelopes. This paper will present a comprehensive approach for establishing new solar envelopes by making use of geometric and radiometric information contained in point cloud data with an integrated environmental performance analysis based on glare and solar radiation.

The present study has a six-part structure. Section 1 will give a general overview of the study. Section 2 will present the theoretical background, which consists of the basic principle of solar envelopes, the potential application of point clouds, and an existing method for creating subtractive solar envelopes. Section 3 will describe the computational workflow of new subtractive solar envelopes. This will be followed by the description of a case study's implementation in Section 4; this description will range from dataset collection to the details of the simulation process. Section 5 will present the simulation results and an environmental analysis that investigated the performance of glare and solar radiation. Finally, Section 6 will offer concluding remarks and suggestions for future research.

2. Theoretical background

This study has proposed a new generation of solar envelopes by making use of the subtractive mechanism with specific consideration to the existing environment's surface properties. In order to elucidate this, three major subjects will be comprehensively discussed: the basic concept behind state-of-the-art solar envelope methods, the potential implementation of point cloud data with geometric and radiometric properties, and the design procedures of the existing subtractive mechanism.

2.1. Basic principle of solar envelopes

In the distant past, there was some form of awareness of the performance of solar access as part of urban fabrics development. This approach can be recognised as part of the ancient world's concept, and it was represented within several cultures such as the Hanging Gardens of Babylon, which were constructed during the Babylonian period (605-562 BCE) [13,14], the El-Lahun village of Egypt (1857-1700 BCE) with its checkerboard urban layout that rigidly implemented narrow north-south streets [15]; and finally, the classical Greek cities of the 4th century BC, which developed solar-oriented homes [16]. Examples such as these not only laid the foundation for the principle of solar access but also contributed to the generation of the solar envelopes that were introduced by Knowles [4]. In a further development, Knowles [5] translated the concept of solar envelopes with considerations of space-time constraints before putting any design parameters in place. According to this principle, solar envelope's parameters can be categorised as both geographic and climatic [6]. Geographic parameters refer to aspects that relate to the spatial relationship between a land

parcel and its surrounding context. These can be physically defined by terms such as longitude, latitude, orientation, courtyard, surrounding facades, sidewalks, building height, floor area ratio (FAR), setback, shadow fences, and streets. In comparison, climatic parameters constitute of non-physical characteristics that are related to the time construction of geometric models; these can be identified by terms such as solar angle, cut-off times, dry bulb temperature, sun path, solar azimuth, solar altitude, and sun access hours. In principle, geographic and climatic parameters correspond inversely to the solar envelopes' volumetric size; that is, the greater the time interval in solar envelope construction, the less solar envelope space is produced.

As illustrated in Fig. 1, daily and annual time settings demonstrate different solar envelope geometries. In a full day setting (Fig. 1-A), the morning sun governs the envelope boundary at the western limits while the afternoon sun establishes the envelope shape at the eastern limit. This setting yields a relatively symmetrical shape that is divided between east and west. This is because of the similarity of their solar altitude angles between 9 a.m. and 3 p.m. On the other hand, the generated envelope for the annual time limit shows moderated steepness toward the north-facing surfaces. This is because the sun's altitude angle is larger in summer when striking the north-facing surfaces.

Furthermore, advancements in the area of computational tools inevitably affect both the workflow of and the method for constructing solar envelopes. Methods of establishing solar envelopes can be subdivided into four categories that are based on both design parameters and computational platforms [6], and are as follows:

- Descriptive geometry—this method involves an intersection between the geometric lines of solar altitudes and the boundaries of the plot according to a predefined period (cut-off-times). The cross-section between these two lines generates a final envelope that fulfils the determined criteria of solar access [17–28].
- Solar obstruction angle—the obstruction mechanism is derived from reference lines within a set of profile angles [29]. It transforms the angle of solar altitude to the solar azimuth that is perpendicularly related to the building façade being analysed during a specific time of the day. As such, the reference lines also include the horizontal property line in the north and the vertical axis of the building within Cartesian space [30–42].
- Constructive solid geometry—this method primarily consists of site extrusion on the basis of solar vector settings. This setting contains rules that will help generate the initial shapes that were extruded from the plot while also taking into account the solar access constraints of the building and its surroundings. Furthermore, the intersection result of these initial shapes generates the final geometry of solar envelopes [7,9,43–48].
- Digital elevation modelling (DEM) —on the basis of image processing techniques, this method quantifies a solar exposure map in order to generate solar volumes [49,50]. This approach simultaneously introduces the concepts of iso-solar rights and iso-solar collections, both of which can be used to implement energy-oriented shapes on urban surfaces.

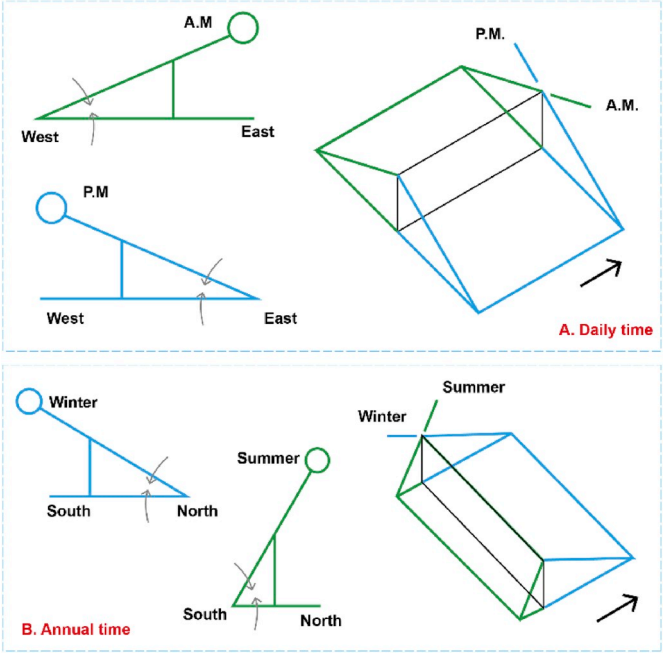

Fig. 1. A design mechanism for establishing solar envelopes, generated from A. Daily time limits and B. Annual time limits. These diagrams are elaborated from a book of Sun, Rhythm, and Form, authored by Knowles [5]. It specifically demonstrates the time setting before 9 a.m., and after 3 p.m. at 34° north (Los Angeles, USA).

These approaches have successfully showcased a progressive trend of implementing solar envelopes as primary components within the architectural design process. During the generation of solar envelopes, these approaches can be categorised into two parts according to the contextual settings. In this case, 'contextual setting' refers to several parameters such as land parcel and surrounding site properties (e.g. vegetation, surrounding buildings, and open space) that might be relevant for generating solar envelopes. Some references properly consider parameters within the local context so that the interdependent relationship between the planned building and surrounding environments can be negotiated [9,17–24,30,33–35,38,48–50]. Meanwhile, others only consider the given plot so that the implementation of solar envelopes primarily focuses on new development areas [7,25–28,31,32,36,37,39–41,43,43–47]. However, the contextual setting of each method needs to be taken into account in terms of design concept and the complexity of the projects due to design parameter variation. Interestingly, the concept of concept has also been used in the recent projects of the Dutch architectural and urban design firm MVRDV: for example, the P15 Ravel Plot, which is located in the Zuidas district, 1082 LC, Amsterdam [51]. This project addresses the idea of solar-oriented design with the integration of a three-dimensional landscape of terraces and greenery. By studying the optimal line of sight and environmental performance, proposed buildings can have open southern exposures with plentiful sunlight.

Furthermore, the rapid development of 3D laser scanning technology has spanned multiple disciplines, especially in the domain of design and engineering. Point cloud data has also become more accessible than ever before, especially forcollecting and processing complex information within an existing contextual environment. While this technology continually improves, a feature of reality-based datasets may provide useful support for the proposed subtractive method of solar envelopes.

2.2. Point cloud data

As a product of laser scanning technology, a point cloud consists of a three-dimensional location with supplementary metadata that corresponds to each measurement record [52]. Similarly, Otepka et al. [53] described each point (P_i) by defining the three coordinates $(x_i, y_i, z_i)^T \in R^3$ and complementing these with auxiliary attributes ($a_{j,i}$) where $j = 1, \ldots m_i$ and i = the number of point attributes. If Pi is a vector $(x_i, y_i, z_i, \alpha_{1_i}, \ldots, \alpha_{m,i})^T$, then the first three components constitute a fixed meaning, like point coordinates, and the other components correspond to a different value for different point entities in the cloud. Another definition was offered by Weinmann [54] who illustrated the entity of a point within Euclidean space (R^D) where D = 2 represents two-dimensional properties such as an image location or a 2D key point while D = 3 indicates a three-dimensional element such as a 3D scanned object. As such, the value of a point can principally be assumed to have no real dimension,

such as length, area, or volume because its dimension equates to a container of points.

According to the above definitions, the data structure characteristics that result in a point cloud can be described further using permanent information. This can be done through the implementation of spatial XYZ coordinates [55] that are followed with supplementary attributes such as colour information (RGB) [56] and reflection intensity (I) ([57, 58]). To identify a specific function for each attribute, its metadata structure needs to be categorised into geometric and radiometric properties [59,60] in the following ways:

- Geometric properties—this characteristic not only facilitates the configuration of the geometrical [61] and visual features of 2D and 3D models [55] but also allows simulation performance to be executed reliably [62]. An interesting example of this can be observed during the development of 3D reconstruction models within the fields of archaeology and heritage [63,64]. In cases such as these, existing buildings have successfully been recreated within 3D models with colour details and representative material characteristics. However, this approach is limited to archaeological projects' contextual scale, which predominantly works with smaller objects, especially when compared to architectural scales. In addition, the modelling procedure from point cloud data to a mesh model inevitably poses a high cost in terms of computational issues. This is a critical matter, especially when dealing with the simulation analysis of complex projects in architectural design practice. For example, a previous study implemented an approach that simulated a descriptive solar envelope method [6]. This method was based on a 3D mesh model created with airborne laser scanning (ALS) datasets. Although this approach has successfully captured more detailed information regarding the site properties of an existing context, it has, unfortunately, presented a major concern for contextual modelling due to the solid modelling process [65,66].
- Radiometric properties—this characteristic refers to the attribute information that is attached to each point within a dataset (e.g. RGB colour and reflection intensity). In addition to typical attributes, this type of point cloud also contains high order attributes or the so-called point feature. In this regard, some authors have defined these features into several categories. For example, Richter [67] developed six identification categories: colour, vegetation, terrain, surface normal, horizontality, and global/local height. In addition to these, Mallet [68] described 27 types of features that are separated into three groups: geometrical features [69], echo-based features, and full-waveform features [70–72]. Unfortunately, these features are only partially applicable to architectural design practices. This is because the amount of effort that needs to be invested in dataset processing makes the process unfeasible. In most cases, its practical application should deal with prior knowledge of technical dataset processing because it only caters to very particular tasks.

Understanding the main characteristics of a point cloud allows for the exploration of more relevant properties in architectural design. This can be observed through several implementations such as building construction [73–75], landscape modelling [76,77], cultural heritage [78–80] and environmental engineering [81–83]. For example, colour information (RGB) can specifically be used not only to identify the inner surfaces of room volumes [84] but also to detect road signage by calculating of hue (H) and saturation (S) values within a dataset [56]. On the other hand, observed reflection intensity primarily deals with the surface and material properties of scanned objects [85] since it contains a return signal strength from laser pulse energy [86]. Thus, this method can be used to identify and map challenging characteristics such as damaged concrete inside tunnels, pavement lines, seafloor stripping, reflective detections signs, and geologic layers [60]. Furthermore, position information (XYZ) plays an essential role in synchronising the coordinate locations of a dataset with various selected values made up of colour and intensity information. This is done so that complex indicated areas can be extracted.

Due to the usefulness of attribute information datasets in point clouds, architects are able to generate environmental performance analyses for proposed architectural designs.

2.3. Subtractive solar envelopes

As a part of the solar form-finding concept that De Luca [9] proposed, subtractive solar envelopes consist of a volumetric three-dimensional matrix, namely 3D polyhedra; this is subtracted based on building facades' required sunlight from surrounding windows (Fig. 2). 3D polyhedra are extruded from a selected land parcel based on a proposed building's criteria, which can encompass width, height, functional utilities, and even the number of floors. In principle, this mechanism has been proven as an effective strategy for dealing with daylight optimisation, direct sunlight, and solar radiation since it capitalises on voxel performance's space tessellation and form generation [87]. In alignment with this approach, Leide and Schlüter [88] developed an analytical and visual methodology through volumetric insolation analysis (VIA) and volumetric visibility analysis (VVA). Their method aimed to embrace the diversities that exist in the urban context combined with various performances such as radiation analysis, airflow, and visibility. Such approaches are also addressed in several references [89–93]. However, these references merely addressthe generative architectural form while neglecting the concept of solar envelopes.

The subtractive simulation process primarily consists of three main stages. *First*, there is window selection per surrounding facades. At this stage, existing facades are selected and subdividedinto window configurations according to predefined criteria, such as dimension and surface grid, which correspond to a particular amount of direct sun access. The selected windows are then represented by centroid points for establishing the sun vectors that are generated from the sunlight hours analysis. *Second*, there are evaluations of the sun vectors that come from the selected windows, affecting the surrounding facades, and the 3D plot, which uses a hit-or-miss procedure. This step involves Boolean intersection with a true or false statement. The statement will be true when sun vectors pass through the polyhedra and false when sun vectors do not hit the polyhedra. This procedure indicates that a true statement will subtract the voxels within the 3D polyhedra while a false statement will contribute to the generation of solar envelopes. *Third*, there is the obstruction index of the remaining polyhedra. The process of ray tracing sun vectors to polyhedra principally generates an obstruction range that is represented by colour-coded voxels. It indicates surrounding buildings' direct sun access obstruction level.

The study will now present a new method for generating solar envelopes by making use of the subtractive mechanism and point cloud attributes.

3. A proposed method for new subtractive solar envelopes

Based on the subtractive method, this study has developed a new generation method for solar envelopes that considers the potential use of point cloud attributes. A series of computational frameworks were formulated to reach this goal (Fig. 3). In general, the proposed method consists of three phases: input, tasks, and output. *First*, **input** constitutes several parameters that construct solar envelopes' geometric shapes and affect performance. It is then divided into climatic and geographic properties. Climatic properties contain a specific location in addition to the indicated periods that are used to calculate solar vectors. Meanwhile, geographic properties include surrounding context parameters that have been obtained from both TLS datasets and the 3D plot of a proposed building (polyhedra generation). These are in addition to the predefined criteria of building height and number of floors. *Second*, **tasks** cater to a set of operations that are performed by calculating and analysing a varied range of inputs from a raw dataset. These operations

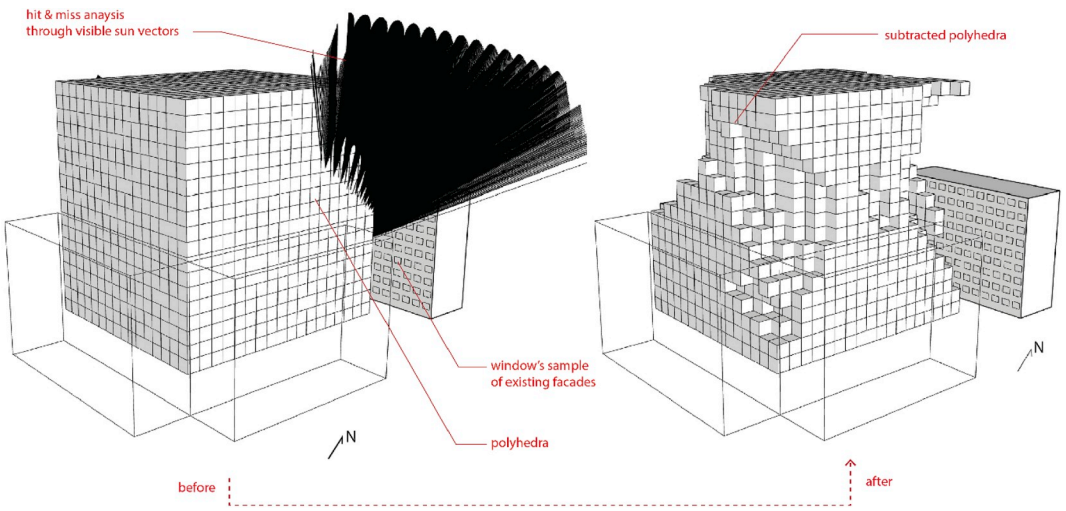

Fig. 2. The design mechanism of existing subtractive solar envelopes. These diagrams are elaborated from the paper of solar form finding, authored by De Luca [9].

involve several off-the-shelf frameworks that have been adapted from existing studies and include factors such as dataset correction, calculation of material properties [12], and the computational procedures of a hit-or-miss analysis for 3D polyhedra [9]. *Third*, **output** consists of the geometric shapes of solar envelopes with an integrated performative analysis based on insolation (solar irradiance) and glare analysis. These analyses aim to evaluate and integrate the environmental performance aspect into the final geometry of solar envelopes. Accordingly, a comprehensive contextual analysis can be performed as decision support for architects during the early design phases. In this case, a simulation of solar radiation would be run to reveal solar energy potential on solar envelopes' geometrical surfaces. This would help architects estimate and identify a new building's solar collector. A glare analysis could be conducted between existing buildings and proposed solar envelopes based on material properties with the goal of avoiding uncomfortable glare as a result of reflective materials on building façades [94].

The proposed workflow employs several supporting tools that cater to the specific tasks in each step. For example, Faro Scene and Cloud Compare (CC) [95] are digital instruments that are used to prepare the raw dataset, which is necessary to create simulation input. Specifically, Faro Scene facilitates scanner-workstation data transfer. This also includes the registration process, colour coding, and clipping box procedures. In comparison, CC is primarily used for dataset preparation. It involves outlier (unnecessary points within a cloud) removal, attribute order selection, point subsampling, dataset formatting, and the scalar field feature, which enables the identification and calculation of point cloud metadata information (e.g. the surface normal of unstructured point clouds and the reflection intensity). Matlab is used to support dataset correction, especially when calculating point clouds' optimal normal values. As a 3D modelling tool, Rhino coupled with Grasshopper is used to simulate solar envelopes. Ladybug (an environmental Grasshopper plugin) [96] is specifically used to calculate direct sunlight hours and perform ray tracing analyses. In general, the proposed workflow uses various dataset formats depending on the tasks and steps that need to be performed. For example, the E57 file is exploited to transfer the 3D point cloud from Faro Scene and CC so that the selected datasets can be interoperable in 3D modelling tools. In alignment with that, the ASCII file is also used to load the 3D point cloud with embedded attribute information. Breps (boundary representation) and TXT files are primarily employed in Rhino and Grashopper to extract or input geometric properties and textual information, respectively.

The proposed workflow was tested by using a hypothetical case study. Each specific task was performed in correspondence with real datasets that were collected using a Faro laser scanner. Section 4 will provide procedural details of the computational workflow.

4. The implementation of the case study

4.1. Dataset collection

The method that this study has proposed was applied to a building context using on-site scanning datasets. At this particular site, the dataset collection needed to comply with several predetermined criteria. *First*, the acquired 3D point cloud originated from terrestrial laser scanning (TLS) datasets. This method aimed to supply accurate geometric properties [97,98] in combination with an attractive, representative 3D model. This can be observed through the inclusion of both the texture and material visualisation of real building contexts which enables view point switching between an intensity format and RGB colour so that attribute value changes can be quickly and easily detected during the dataset preparation in a point cloud environment. In comparison between ALS and TLS datasets, it is crucial to note that TLS can cover a wide range of surrounding elements from isolated areas. These contextual elements include vegetation, temporal site objects, and other properties that are potentially relevant for solar envelope simulation. *Second*, attribute information should at least include the properties of position information (XYZ), colour information (RGB), and reflection intensity (I). These attributes play a great role in dataset correction and calculating material properties for the environmental analysis of solar envelopes. This study specifically collected a sample of 3D point cloud data located in the Faculty of Architecture, TU Delft, Delft 2628 BL, the Netherlands. Geometrically, the selected dataset consisted of building facades, ground areas (pavements), vegetation, and surrounding buildings and objects. This dataset was harvested using a Faro Laser Scanner Focus S350. As a long-range scanning application, this tool not only supports extended distances and precise angular accuracy but also facilitates on-site data quality optimisation. The tool's main technical specifications are as follows (see Table 1):

The harvested dataset consisted of five single scans in order to capture the facades of the architecture faculty building and its surroundings (Fig. 4). Each scan was taken within less than 6 min. The approximate scan size was 10240 × 4267 Pt with a point distance around 6.1 mm/10 m. This setting yielded a point density of around 22 million points for each scan.

4.2. The computational design process

As illustrated in Fig. 3, the proposed method is divided into four sequential design process, each of which consists of different tasks depending on the type and level of information received from the input section. An in-depth discussion of each step is given below.

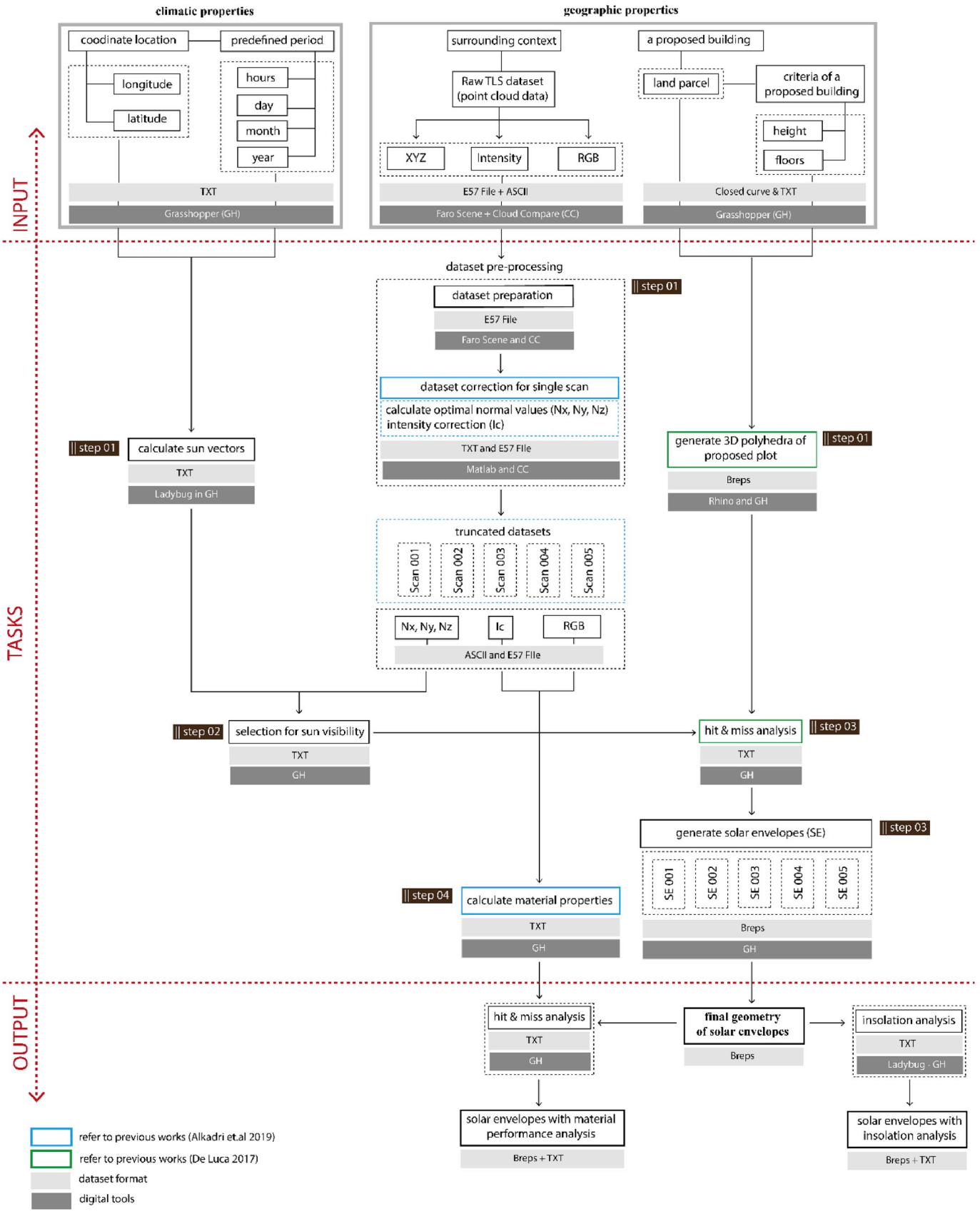

Fig. 3. The computational workflow used in the proposed method of generating new subtractive solar envelopes.

Table 1
Technical specifications of the tools [99].

No	Parameters	Performance specification unit
1.	Ranging unit	
	Range	0.6–350 m
	Ranging noise	@ 10 m–0.3 mm (90% reflectivity)
	Range error	±1 mm
	Angular accuracy	19 arcsec for vertical/horizontal angles
	3D position accuracy	@ 10 m–2 mm
2.	Colour unit	
	Resolution	165 megapixels
	High dynamic range (HDR)	Exposure bracketing 2x, 3x, 5x
3.	Laser	
	Laser class	Laser class 1
	Wavelength	1550 nm
	Beam divergence	0.3 mrad(1/e)
	Beam diameter at exit	2.12 mm (1/e)
4.	Extended operating temperature	−20° - 55 °C
5.	Humidity	Non-condensing

4.2.1. Step 01

This step contains several parts that can be simultaneously performed. This is due in part to different preliminary inputs. *First*, the calculation of sun vectors requires a specific coordinate location and a selected period. In this case, the position of Delft is located at latitude 52.0116° N and longitude 4.3571° E. The time setting takes a sample of the required period on the 21st of each month, ranges from January to July, and starts between 9 a.m. and 6 p.m. This setting yields a total of 16 sun vectors that comprise the selection of the visible sun. *Second*, the pre-processing step caters to the two aspects of dataset preparation and scan correction for each scan. Essentially, this step enables architects to not only filter important information from the raw dataset but also identify parameters that considerably influence the values of metadata properties during scanning. These parameters can originate from environmental and meteorological factors, atmospheric pollution [100,101], and scanning geometries [102]. To minimise the effects of these conditions, tasks are performed to prepare the selected dataset. For example, removing outliers removal and clipping boxes both determine and clean dataset boundaries (Fig. 5). These outliers usually arise when scanning objects using a 3D laser scanner. This is due to the varying point densities and measurement errors that are experienced during scanning. In addition, sub-sampling procedures are applied to each scan in order to manage dataset point density by setting the distance between points to 5 cm. On average, this step produces 200.000 total points for each data scan.

After the selected dataset is prepared, the correction procedure is applied to each data scan. This specifically aims to correct the erroneous measurements within dataset attributes that have been generated due to noise interference in sensors, equipment sensitivity, laser wavelengths, and by targeting the surface geometry [103]. In this specific case, dataset correction involves the calculation of optimal normal values (Nx, Ny, Nz) and intensity correction (Ic). These normal values are calculated to find the average distribution of points that constitute a good projection as created by the laser beam during scanning. This is because the scattering condition of points corresponds differently at certain angles. This requires that the surface normal of datasets be identified first. Accomplishing this means applying the Hough Normal plugin [104] to each scan because of the unstructured cloud of points. In alignment with the previously stated requirements, the distribution of points is plotted by simulating different cosine values that have been extracted from various angles of incidence, which range from 10° to 90° (Fig. 6-A). This step is performed using the following equation [103] and taking into account the original location of the laser scanner at (0,0,0):

$$i = \cos^{-1}\left(\frac{\overline{dn}.\ \overline{dl}}{|\overline{dn}||\overline{dl}|}\right) \tag{1}$$

where i = incidence angle.

$\overline{dn}$ = direction of the surface normal.

$\overline{dl}$ = direction of the laser pulse.

Afterwards, the distribution of point density is evaluated by calculating a standard deviation of cosine values within the dataset (Fig. 6-B). Thus, the discovered scattered points are removed and the densest is truncated. As a result, each data scan shows a different number of truncated points depending on the density level of datasets within the plot of cosine values. These truncated datasets consist of optimal normal values that can be used for intensity correction and the calculation of sun visibility, which will be explained in the second step.

In principle, intensity correction is performed to calculate nearly 'true' values of intensity from the raw dataset (Fig. 7). According to Kashani et al. [60], intensity information is influenced by several fig-ureparameters such as the behaviour of the target surface, acquisition geometries, equipment and environmental factors. However, some local constraints, such as climatic condition (moisture and temperature pressures) and tools' default settings during scanning, make the full correction of these parameters impossible to perform. Accordingly, this study performed intensity correction by only taking the relevant and significant parameter, such as the angle of incidence (α) to the TLS dataset. The following equation [60] was used for intensity correction:

$$I_c = I_{raw}\ \frac{1}{\cos\ \alpha} \tag{2}$$

where I_c = corrected intensity.

Fig. 4. Dataset collection and the different views captured in relation to the scanning position.

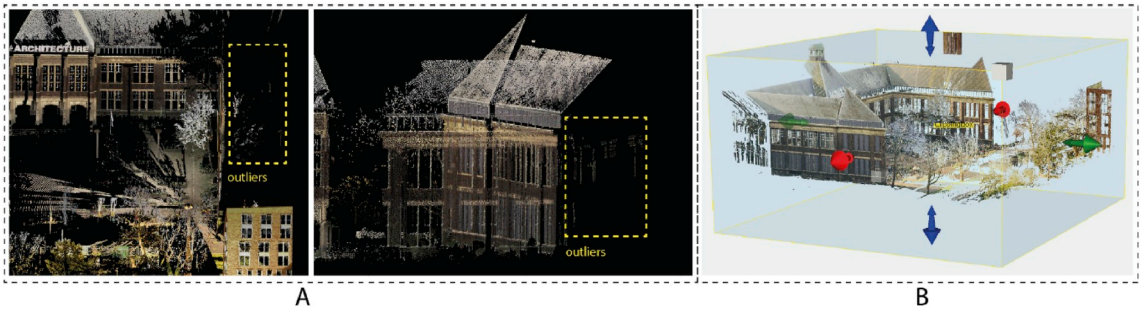

Fig. 5. Dataset preparation A. Outlier removal B. Clipping box.

I_{raw} = original intensity.
α = angle of incidence.

As illustrated in Fig. 7, the dataset transformation that resulted from intensity correction employed four colour steps. The colours ranged from blue, which represents the lowest intensity value, to yellow, which represents the highest intensity value and refers to the most reflective surface. Dark and light green are intensity colours that straddle the threshold. The following results describe the distribution of the intensity datasets:

- In general, a major discrepancy between initial and corrected intensity can be observed primarily in roof areas and in some minor parts in building walls (see part of the scalar field intensity). The predominant intensity colour changes from dark green (in the column of raw intensity) to yellow (in the column of corrected intensity). This transformation is principally affected by spectral reflectance and oblique surfaces. In this case, the material on the building's roof consists of smoother surfaces (copper roof) than the material on the building's wall (old brick). Spectral reflectance on a smooth surface returns the same incident energy to the scanner due to the mechanism of specular reflection [105]. The same rule also applies to the oblique position of the building's roof in relation to the scanner's location. The backscattering intensity of a laser beam is greater on oblique surfaces than on direct surfaces [60].
- According to the intensity distribution values (from the raw intensity to the corrected one), all scans show a similar statistic regarding the increasing values of yellow (high reflective surfaces) while other colour intensities are distributed dynamically depending on the data scan. For example, dark green and blue show a similar pattern regarding the increasing (Scan_001 and Scan_004) and decreasing values (Scan_002, Scan_003, and Scan_005). Meanwhile, light green has more scans with decreasing values (Scan_001, Scan_003, and Scan_004) than increasing values (Scan_002 and Scan_005). Identifying colour intensity on these scans enables us to not only create a clear boundary between a different range of values but also more deeply understand the characteristics of surface material properties in the existing building.

Third, the polyhedra act as a proposed building's 3D envelope (Fig. 8). The envelope is built according to the new building's relevant criteria such as width and height, functional utilities, and number of floors. Principally, each polyhedron represents a typical room in the real building. In this scenario, it consists of $3 \times 3 \times 3$ m with the total number of polyhedra being equivalent to 180 rooms. The polyhedra are then placed in the courtyard of the faculty building so that the spatial relationship with the surrounding buildings can be examined. A proposed building's function should support academic environments, thus including, for example, space for meeting rooms, a library, and staff offices.

4.2.2. Step 02

In principle, the calculation of sun visibility aims to identify visible sun vectors that are not violated by existing buildings and surrounding properties. This requires that the sun vectors from the indicated period be multiplied by optimal normal values that have originated from truncated points in each data scan. In order to identify points that meet sun visibility criteria, the calculated vectors are filtered by considering only those values that are smaller than 90°. This is because sun vectors with angle values that are equal to and larger than 90° are not visible to the scanned point. Ultimately, the procedure results in a group of points within each data scan that meet the criteria of the visible sun vectors.

4.2.3. Step 03

This step calls for the performance of a hit-or-miss analysis that requires input from selected points in the second step and the 3D polyhedra in the first step (Fig. 9). In this case, 16 sun vectors continuously evaluate the 3D polyhedra over 1008 h. This procedure is subsequently run on each data scan, resulting in a different number of ray intersections. With a Boolean operation, each polyhedron is automatically transformed into a voxel and assigned the true or false criteria. Voxels with 'false' values are indicated as obstruction indexes that need to be eliminated. These obstruction indexes can be viewed as green dots attached to the polyhedra (see Fig. 9, specifically part of the obstructive points). Meanwhile, 'true' values are used to generate solar envelopes. This is predominantly illustrated in yellow boxes (see part of selected voxels for solar envelopes) with a different number of voxels for each data scan.

Based on Fig. 9, some analysis elements can be further discussed as follows:

- Scan_004 illustrates the highest number of voxels that ultimately meet the criteria of solar envelopes while Scan_001 and Scan_003 show the least. This trend demonstrates that the densest points are involved in ray tracing analysis, and the smallest number of voxels are produced. This can be observed on the intersection lines of Scan_001 and Scan_003; they nearly cover the polyhedra, especially when compared to the other scans. These intersection lines are principally affected by the density of existing site properties and the number of truncated datasets that generated correction. On the other hand, it can be argued that increasing site properties (e.g. tress, adjacent buildings, and other elements) during simulation can significantly reduce the total voxels for solar envelopes. However, in this case, dataset correction plays an important part in filtering optimal normal values from the dataset, which means that not all points are available for use. Moreover, the step of sun visibility guarantees that only relevant points that meet the criteria of visible sun vectors may proceed to ray tracing analysis.
- The generated voxels for solar envelopes consist of colour-coded values. Sequentially, these go from yellow to green, indicating the level of obstruction from low to high. As illustrated in Fig. 9, most of the data scans show yellow and light green voxels, meaning that, for the indicated period, only some are dark green in Scan_004. It follows that the remaining voxels can be further synchronised with a proposed building's functional program.

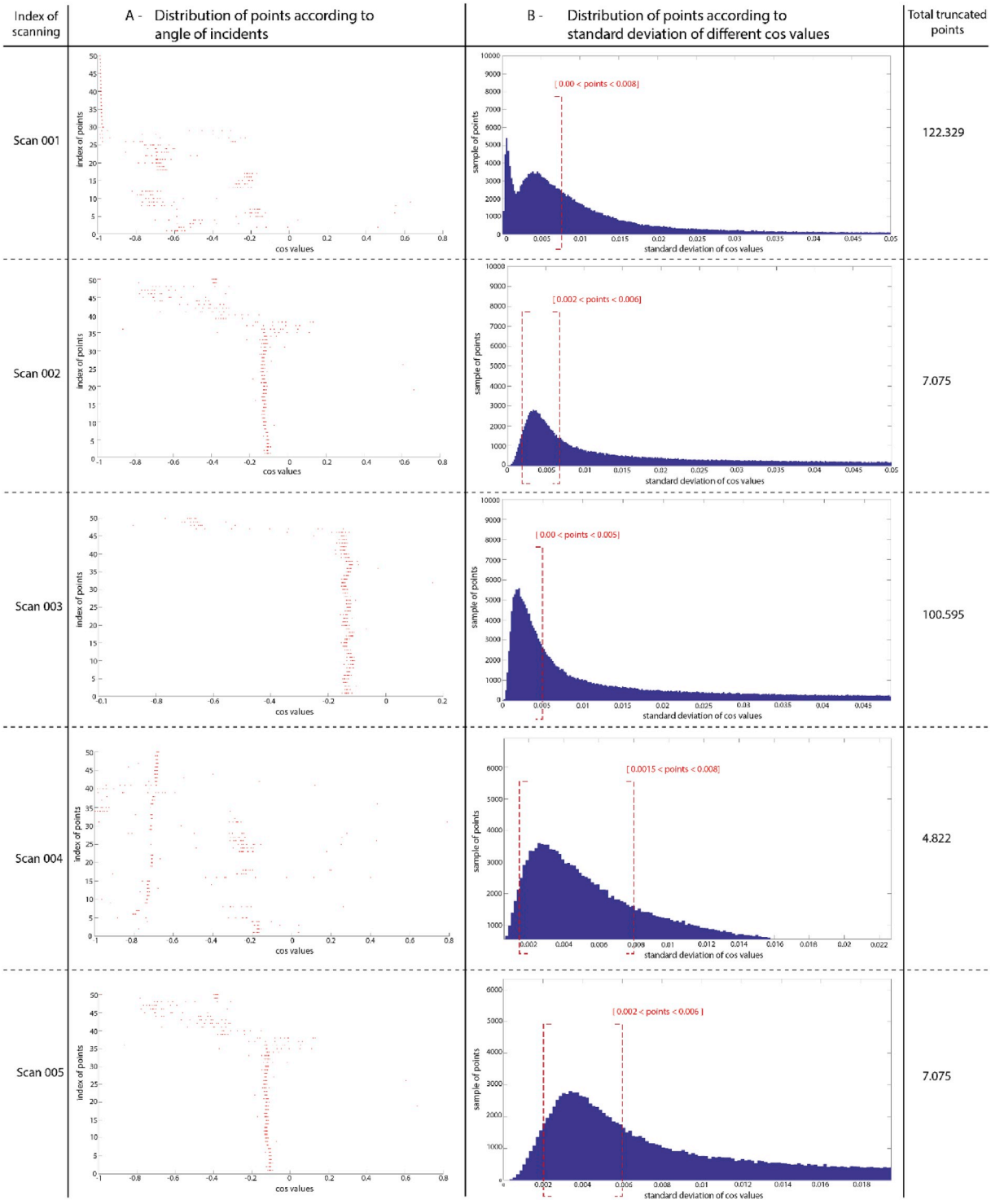

Fig. 6. The distribution of points on each data scan according to A. Angles of incidence and B. The standard deviation of different cos values.

- With regard to the geometrical configuration of generated voxels, each data scan shows a different voxel composition depending on the distance between the polyhedra and the surrounding facades. In this case, obstructive points that were generated from ray tracing affected most polyhedra facades that faced the scanner's position.

4.2.4. Step 04

As a part of environmental performance simulation, this step calculate the material properties of existing buildings as extracted from the point cloud data. A glare analysis between the final geometry of the solar envelopes and the existing buildings is also performed to identify voxels that might be affected by certain material properties. Given that radiometric information (RGB colour and corrected intensity) is collected from the point cloud data, the material properties are calculated according to the thermal (albedo and emissivity) and optical parameters (reflectivity and translucency). As Fig. 3 showed, the detailed procedure for the calculation of material properties has been extensively addressed in previous research [12]. Accordingly, the present study mainly focused on integrating materials workflow into the computational framework of solar envelopes.

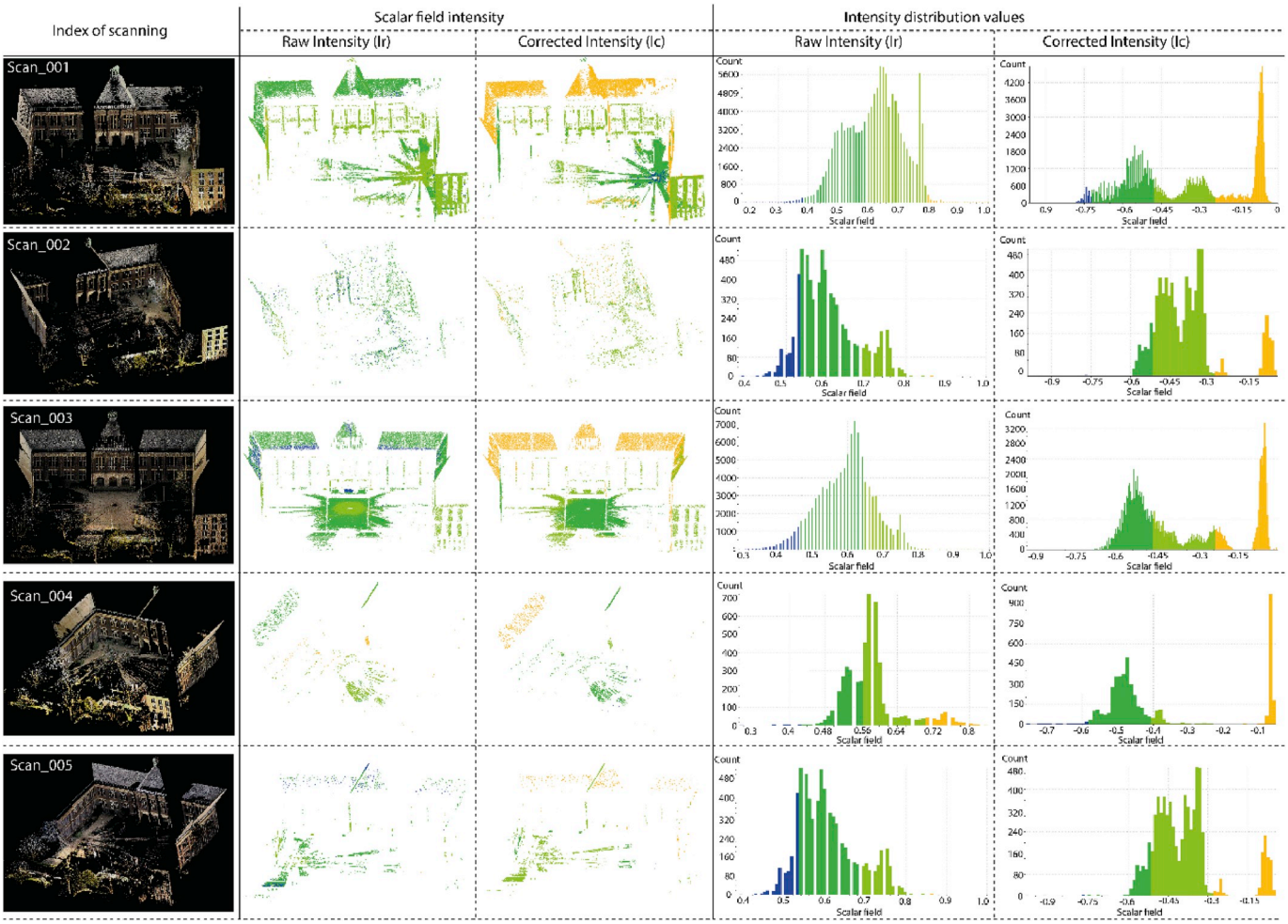

Fig. 7. Intensity correction on each data scan.

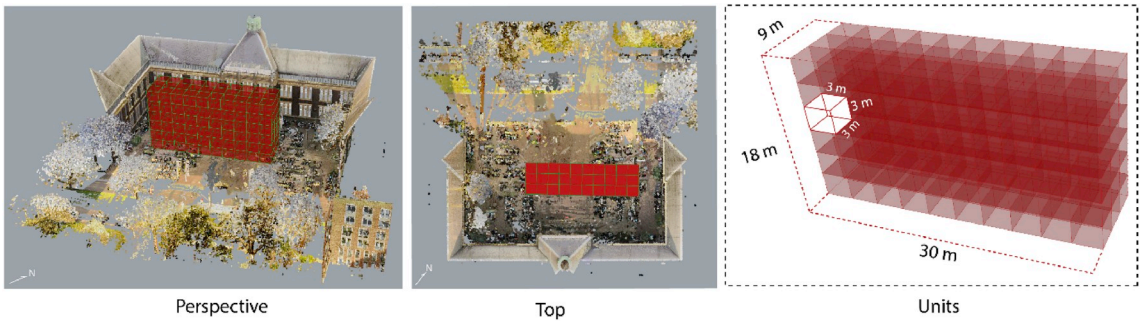

Fig. 8. 3D polyhedra of a proposed building.

Furthermore, the calculation of material properties was performed on the sample of data scans. In this case, Scan_003 was selected to illustrate the result of material distributions because its scanner position was located in the centre of the selected site. This was done so that dataset coverage could be evenly captured on all sides of the building (Fig. 10). Setting the threshold value of material properties in a range of 0.0–1.0 allows for the density of points in each material property to be calculated. In addition, the resulting areas can be visually illustrated within the dataset.

Fig. 10 shows that all material properties illustrate a similar trend regarding the point density of the smallest and largest values. For example, the smallest values with a point density of less than 1% can be identified in several ranges within one material property, such as albedo and reflectance, with three property ranges, and emissivity and transmissivity with 4 and 2 property ranges, respectively. Within these ranges, only the threshold values of 0.8–0.9 and 0.9–1.0 illustrate an equivalent range in all material properties. In this case, the range of 0.9–1.0 shows that albedo and average reflectance have similar 0 values. This is also in alignment with the trend exhibited by the largest value point density. With a value of more than 20%, albedo, reflectance, and emissivity constitute the same range at 0.5–0.6, consisting of 20.9%, 21.83%, and 36.36%, respectively. With regard to the surface distribution of these properties, the range of 0.5–0.6 predominantly covers ground areas around the scanner position with additional areas on the

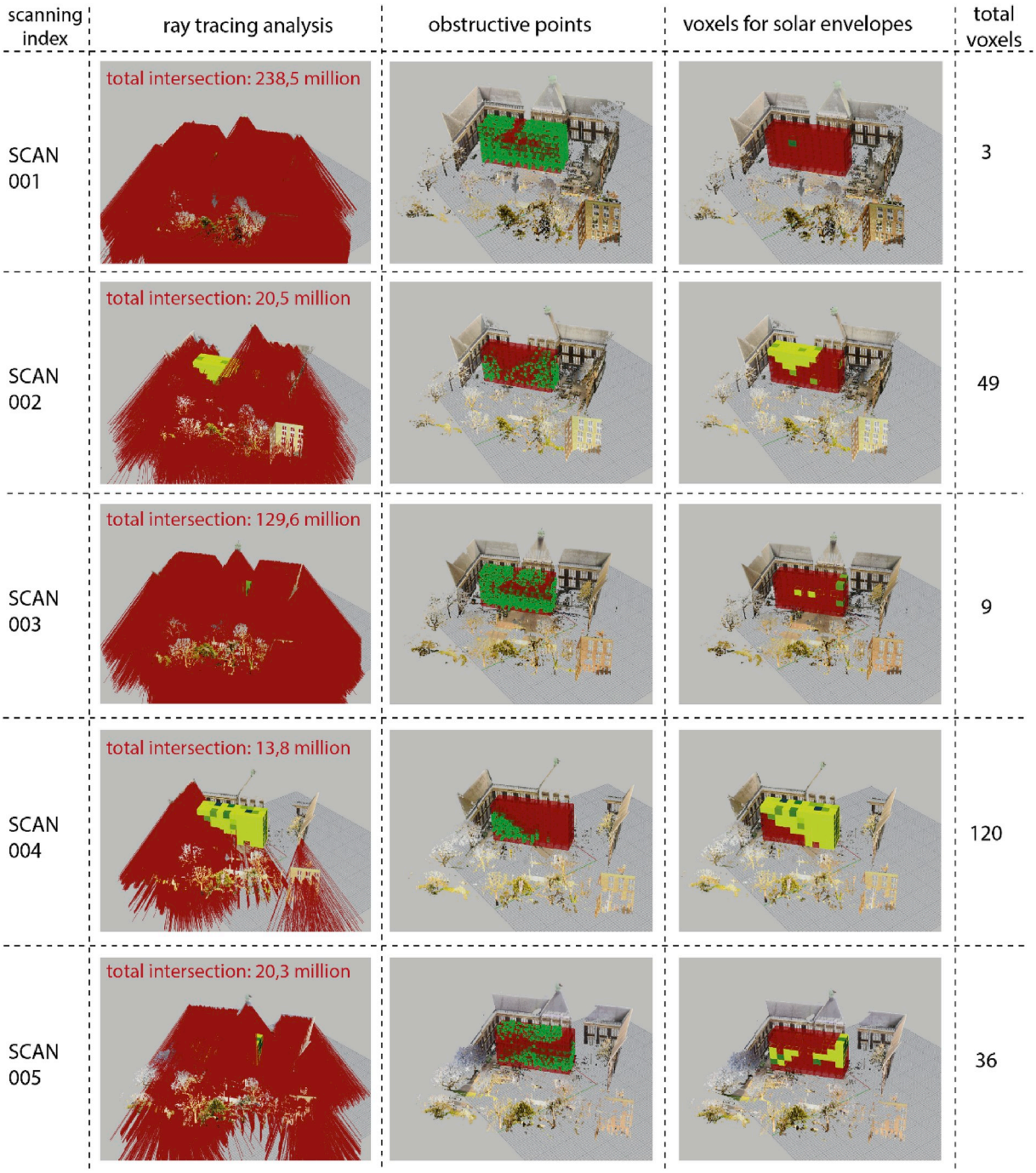

Fig. 9. Hit-or-miss analysis for each data scan.

building roof for the albedo and reflectance property, and the building wall the emissivity. Meanwhile, for transmissivity, the largest value of the property range is found within the ranges of 0.2–0.3 and 0.3–0.4. Identified areas are primarily scattered around the building roof and the ground. In general, this surface material catalogue enables architects to identify particular areas within the dataset based on certain property thresholds so that the surface characteristics of the existing context, especially the ones that are related to the material performance of specific areas, can be better understood.

5. Results and discussion

The present work has articulated the research in three main parts. The first part described the geometric configuration of solar envelopes as a final output of the simulation result. This solar envelope was subsequently followed by an environmental performance assessment that the other two parts addressed. These parts aimed to investigate the potential and impact of the geometric solar envelopes as it pertains to both the building and its surroundings. This involved an insolation analysis on the final solar envelopes and a glare simulation based on material properties. A sequential in-depth discussion of these parts is presented below.

5.1. The final geometry of solar envelopes

Having created solar envelopes for each data scan, the resulting

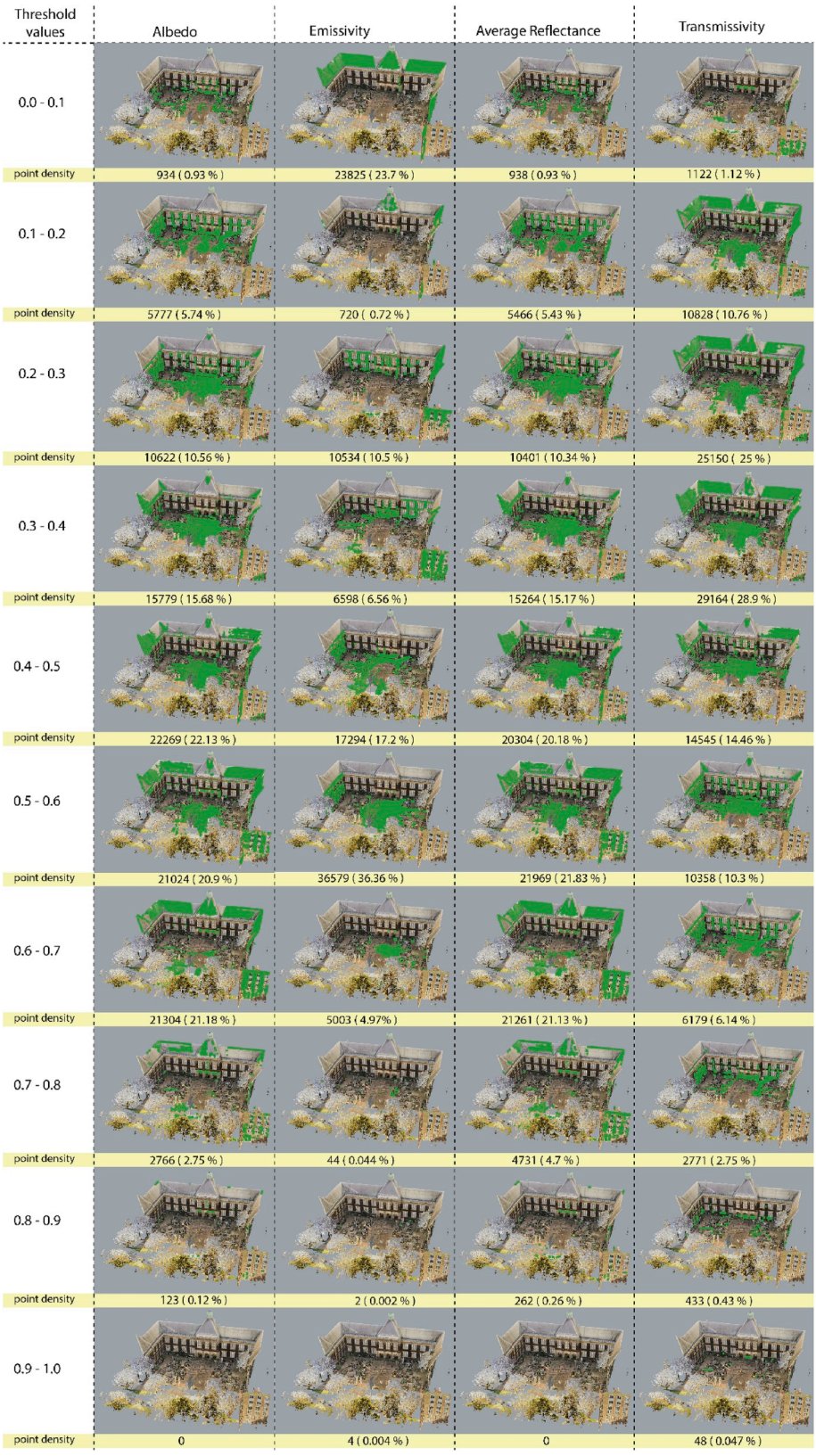

Fig. 10. The surface distribution of material properties in Scan_003.

geometries can ultimately be combined into single envelopes within the completed datasets of the surrounding context (Fig. 11). In total, it consists of 217 voxels due to overlapping envelopes from all data scans. However, after overlapping envelopes are removed, the number of final envelopes is reduced to 133 voxels. Based on Fig. 11, some analytical conclusions can be drawn as follows:

- The final geometry of solar envelopes principally acts as a geometrical core that fulfils the criteria of solar envelopes. Accordingly, additional voxels that are generated beyond the volumetric size of initial envelopes can still be a part of solar envelopes as long as the indicated voxels fit the required number and plot of the 3D polyhedra (the proposed design). Therefore, architects can simultaneously consider the functional program and related activities that correspond to the intended voxels.
- In order to identify the distribution of overlapping voxels from all data scans, the combined solar envelopes were plotted with colour-coded attributes. The final voxels were divided into three colour ranges: dark, medium, and light red. *First*, voxels with a dark red colour illustrate the highest level, consisting of at least more than two overlapping envelopes. This indicates that those voxels have successfully fulfilled the solar access criteria of several data scans. Accordingly, the selected voxels can be prioritised in order to fulfil the main activities of the building that require fulltime sun access during the determined period such as those buildings that contain meeting rooms. *Second,* the voxels with a medium red colour consist of two overlapping envelopes. These voxels can be fulfilled with any functional programs that do not require a full day of sun access criteria, such as staff or work rooms. *Third,* light red voxels might be relevant to the building's tertiary or supporting activities, such as open space, corridors, and service areas.
- In general, voxel distributions in each colour range are not only varied in terms of the quantity, but are also diverse in terms of geometric configuration. In this case, the light red category constitutes the largest volume of envelopes with 66 voxels followed by the medium and dark red categories with 52 and 15 voxels, respectively. This indicates that the geometric characteristics of each data scan may considerably affect the number of identified voxels within the combined solar envelopes. Moreover, an interesting pattern can be observed in the vertical geometry of stacked voxels that can be assumed as equal to building floor levels. The light red voxels nearly fulfil space on the first, second, and third floors while the voxel distribution of the medium one mainly concentrates on the fifth and sixth floors.

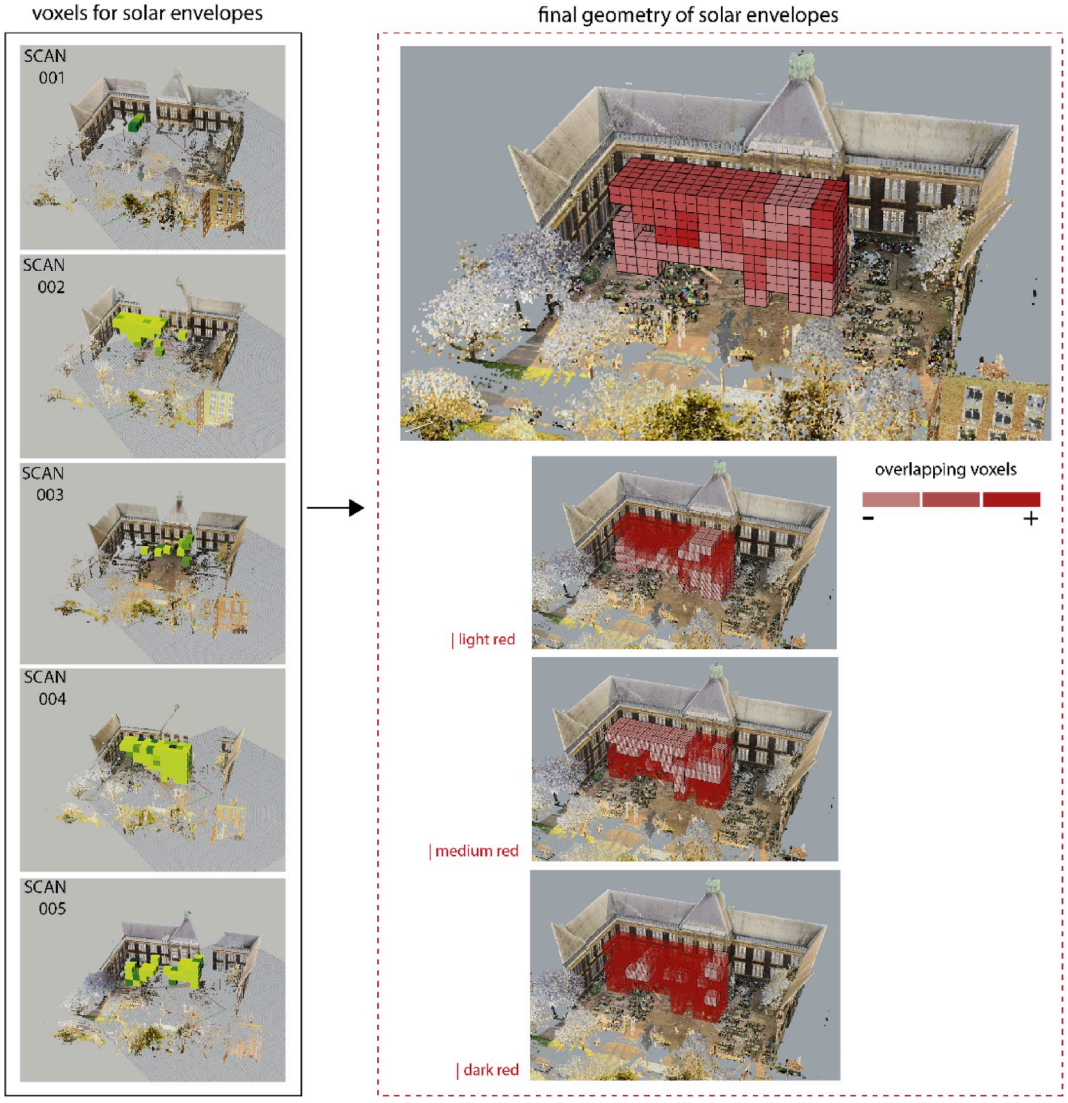

Fig. 11. The final geometry of solar envelopes.

5.2. Insolation analysis for solar envelopes

In principle, insolation analysis performs an integrated environmental assessment on the final geometry of solar envelopes that focus on solar radiation. The objective is not only to identify and calculate the potential of solar energy that can be permeated by a geometric surface of solar envelopes but also to illustrate for architects how integrated environmental analysis can be achieved through this approach. Accordingly, architects can draw a sustainable impact for future scenarios regarding buildings and their surroundings.

Furthermore, the simulation of solar radiation employs a trigonometric principle by calculating cosine values between the surface normal of each voxel and solar vectors that are originated from climatic properties (Step 1 in Fig. 3) [106]. In this case, only positive cosine values are considered because of the inability of surfaces to absorb negative amounts of energy when dealing with incident angles over 90°.

As shown in Fig. 12, all scans illustrate a similar trend regarding the surfaces that have the most potential for collecting solar energy, which are north-facing facades. This is because the location of existing buildings creates a massive obstruction to direct sun access for the south-facing facades of solar envelopes. In addition, the site is characterised by a low solar elevation angle due to its location's high latitude. This condition makes the surfaces of solar envelopes inaccessible in terms of receiving direct sun access, especially when there is close proximity to surrounding buildings. Thus, north and west-facing façades are identified as potential surfaces for the placement of solar collectors or the implementation of passive heating strategies.

Ultimately, the resulting values of insolation analysis show that the entire surface of solar envelopes reaches around 844 kWh/m^2 during a predefined period. For comparison, this amount of energy can be used to supply an average Netherlands household with electricity for around 2.89 months [107]. Therefore, this result should spur architects to internalise a good recommendation, enhance environmental awareness, and make better design decisions in future planning. Nevertheless, the

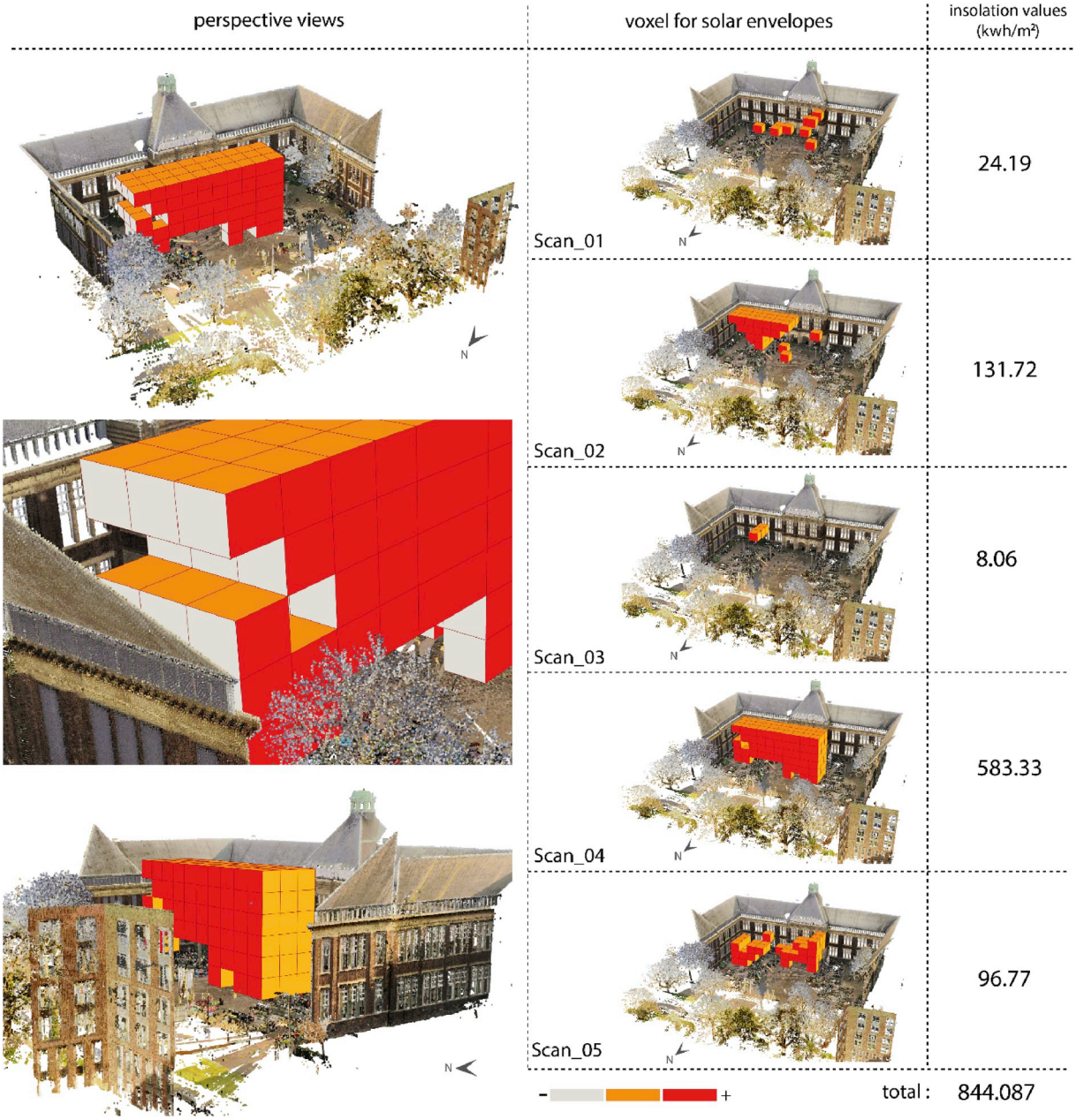

Fig. 12. The insolation analysis of the final solar envelopes.

proposed insolation analysis would benefit from further consideration with regard to the parameters that are involved in the calculation, such as diffuse and reflected radiation [108], air mass, temperature, and other environmental factors.

5.3. Glare analysis simulation

Before performing a glare analysis between the final geometry of solar envelopes and the identified material properties of the existing context, two selection criteria must be set, namely selected points based on sun visibility and normal vectors based on specular reflection. *First*, this criterion employs a similar mechanism as in the second step in Subsection 4.2 (part of computational design process). In this regard, the threshold values of material properties only consider selected points for extraction from the sun visibility selection. As a result, the number of points registered in all material properties decreased significantly due to incompatibility with the visible sun criteria (Fig. 13). The largest discrepancy (before and after the sun visibility selection) illustrated a similar trend among the material properties, especially for albedo, emissivity, and average reflectance. These properties constituted the same value range of 0.5–0.6, similarly consisting of more than 17 thousand points, while transmissivity was identified at value ranges of 0.2–0.3 and 0.3–0.4. Regarding the surface distribution of the dataset, most of the identified values after the sun visibility selection were located on the building's roof with a significant decrease in the ground areas. This suggested that the sun vector of points located on the ground level predominantly consisted of zero and negative values, meaning that those points were automatically filtered by the criteria of visible sun.

Second, sun vectors that were acquired from the selected points and threshold values of material properties were simulated by considering specular reflection. This was done by assuming that the angle between the normal vector and the incoming light was equal to the one between the normal vector and the reflected light. This requires that sun vectors around the point normal be rotated to 180°. Furthermore, the selected vectors and points were carried forward to the hit-or-miss analysis step with the final geometry of solar envelopes.

5.4. The geometric configuration of solar envelopes based on glare simulation

This section discusses the result of glare simulation between the proposed solar envelopes and the existing buildings on the basis of material properties. Since this simulation adopted a similar mechanism as the sun visibility criteria, its procedure was therefore limited with regard to the geometric intersection between the solar envelopes and the sun vectors reflected from the surroundings. The simulation result primarily identified affected geometries within the solar envelopes without considering the luminance level of reflected lights. Architects can use this approach to avert proposed building's microclimate issues by considering material performance during the conceptual design stage.

As shown in Fig. 14, the geometric configuration of the identified voxels have a similar pattern for specific ranges of thresholds. For example, a zero voxel is predominantly identified at the range of 0.8–1.0 except for the transmissivity property, which refers to the range of 0.0–0.2. This value means that the reflected light from the surroundings fails to intersect with the geometry of the solar envelopes due to a different incident angle and point density (refers to Fig. 13) within the performed threshold. In addition, the emissivity had a different pattern when compared to the others. This is because emissivity refers to the intensity values within an inverse range. Consequently, it affects the calculation of other properties. The indicated patterns are listed as follows:

- Emissivity consists of three zero voxels (in a range of 0.7–1.0) while others only consist of two zero voxels (albedo and average

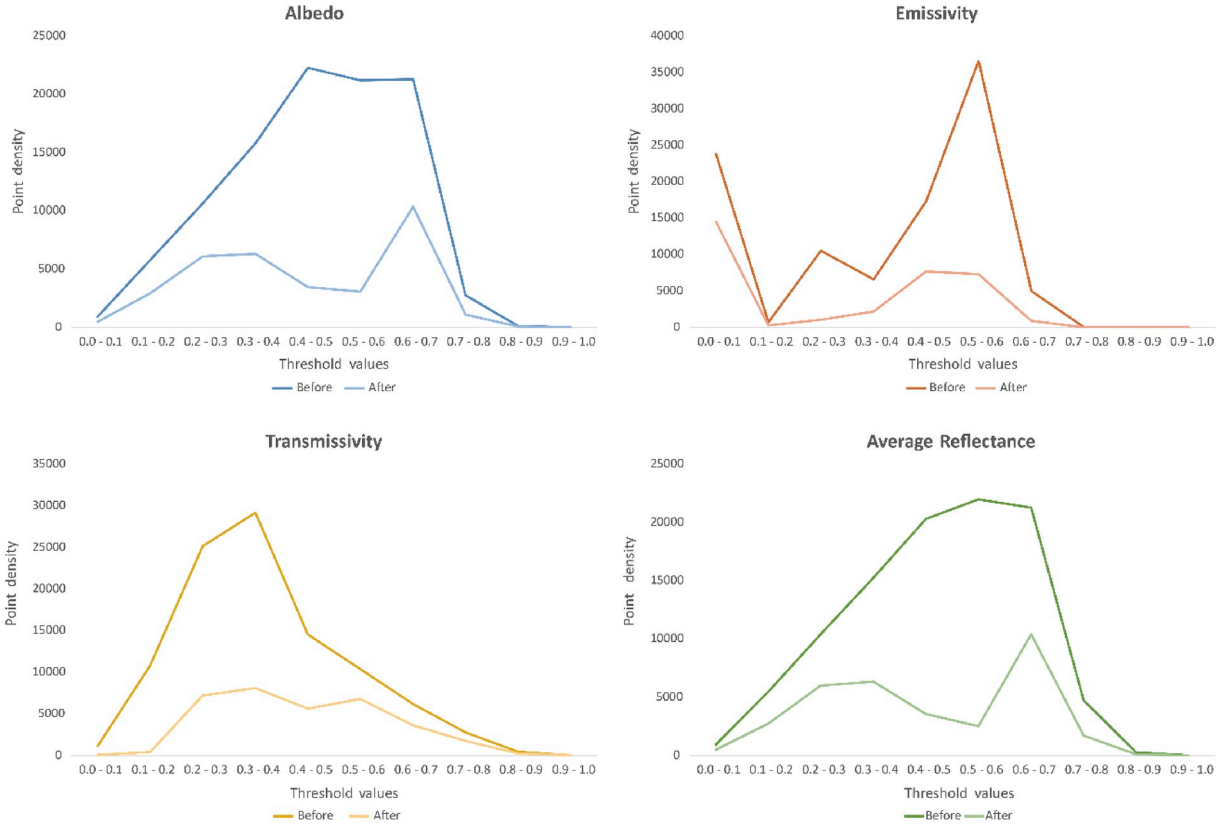

Fig. 13. A comparison of material properties before and after the sun visibility selection.

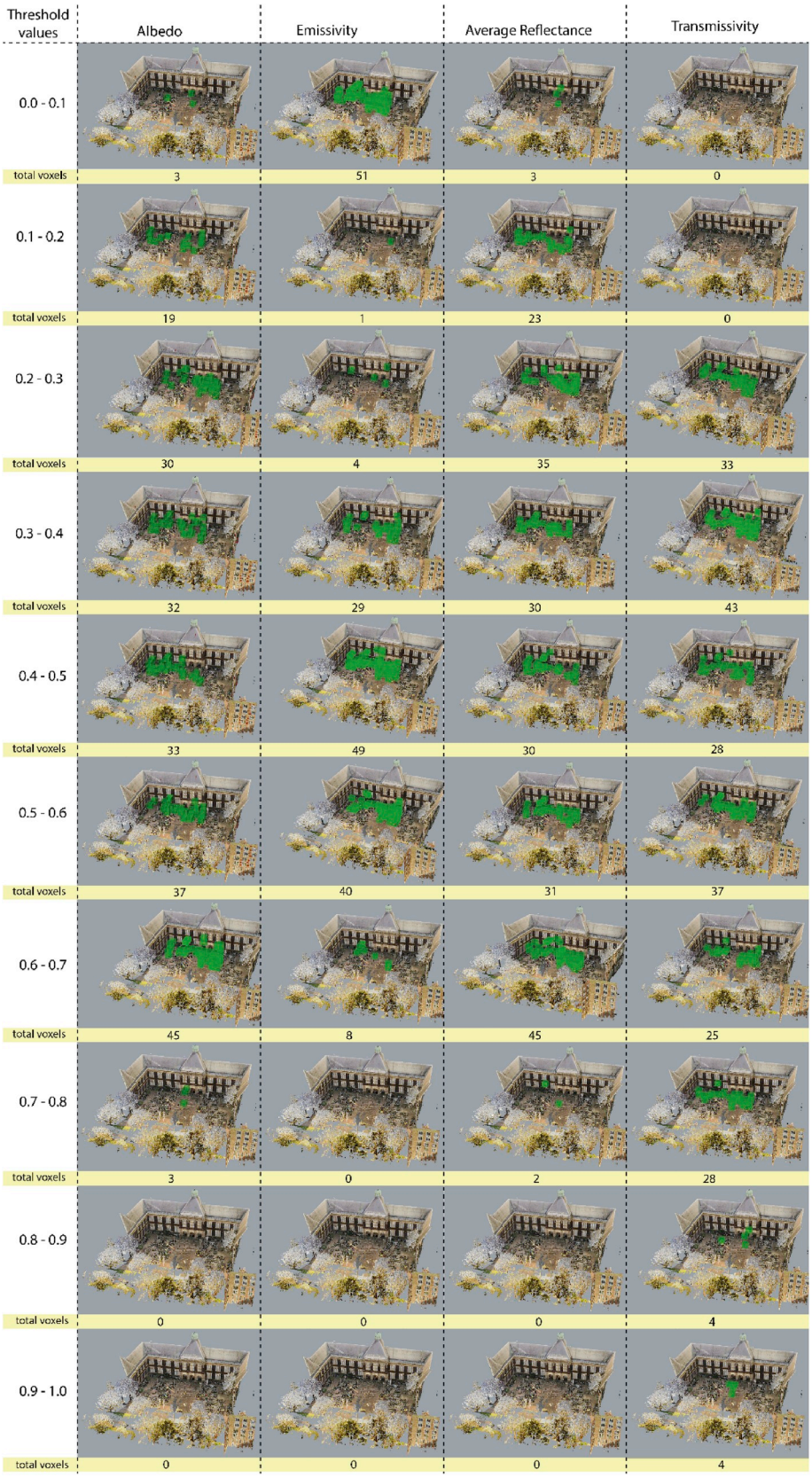

Fig. 14. The geometric configuration of solar envelopes according to glare simulation analysis.

reflectance, similarly in a range of 0.8–1.0, with transmissivity in a range of 0.0–0.2).
- With regard to the distribution of the voxels, all properties contain four threshold ranges for registered voxels, amounting to less than ten, except for emissivity which consists of six ranges.
- Emissivity results show significant contrast in terms of the quantity of identified voxels in comparison with others. This can be observed in ranges of 0.0–0.1, 0.2–0.3 and 0.6–0.7.

6. Conclusions and future recommendations

This study has built on a novel method of generating subtractive solar envelopes that are based on the attribute information found in 3D point cloud data. The present workflow has confirmed the feasibility of integrating both geometric and radiometric properties of a point cloud, especially when supporting the contextual analysis of a proposed building. In particular, point cloud data acts as a basis for making an informed design context, therefore allowing environmental performance to be embedded in the workflow that is associated with the development of new solar envelopes. This approach ultimately allows architects to not only compensate for missing information during site analysis but also identify the context's microclimate conditions during the preliminary design stage. In general, this work warrants several remarks, which are listed as follows:

- With the overarching goal of developing new subtractive solar envelopes, attribute information in a point cloud enables the expansion of the functional properties that are available with 3D scanning technology. This is important in the architectural design stage, especially when dealing with environmental performance analysis, since it provides an alternative to focusing exclusively on 3D reconstruction and data visualisation.
- Dataset correction is necessary not only to obtain a point cloud's corrected optimal normal values but also to minimise erroneousness in datasets during scanning. This will also help architects select relevant information to comprise the input that is needed to develop solar envelope simulations.
- Integrating aspects of material properties into the new workflow of subtractive solar envelopes will help contribute to the expansion of performance analysis in the relationship between new buildings and their local contexts. This also supports architects in more appropriately configuring any activities that are suitable, especially with regard to the solar and material performance of certain voxels and activities that need direct solar access within a certain period.

Acknowledging the limitations of this study, there are some elements that would benefit from further consideration. For example, the computational issues that were experienced during simulation were created by highly dense datasets, and this remains a major concern. Some of the study's aspects merely require very particular adjustments, such as the number of sun vectors or the point density of datasets. Moreover, synchronisation between more existing urban properties and different functional utilities may affect solar envelopes' final geometry.

In further research, some potential aspects can be explored by investigating the relationship between the floor plan and an optimised layout design for both solar envelopes and energy efficiency. This will allow architects to define the layout configuration for each voxel within solar envelopes given that solar envelopes are based on the direct solar access that is available in a specific timeframe (per hour and per day). Moreover, the proposed method can be explored using different climatic contexts, such as tropical climates, as doing so can potentially expand possibilities for implementing designed solar envelopes within different urban settings.

Declaration of competing interest

None.

Acknowledgements

We thank Indonesia Endowment Fund for Education (LPDP) for funding a PhD Research of the first author under the chair of Design Informatics, Faculty of Architecture and the Built Environment of TU Delft, the European Regional Development Fund grant (the Estonian Centre of Excellence in Zero Energy Resource Efficient Smart Buildings and Districts) ZEBE n. 2014-2020.4.01.15-0016 and the European Commission H2020 grant Finest Twins n. 856602 for supporting the work of the second author. In addition, the authors would like to express their gratitude to Marnix van der Wolk from Faro Benelux B.V. for providing access to the dataset, Yu-Chou Chiang for his technical support during dataset processing, Professor Knowles and the MIT Press for providing access of images copyrights regarding the concept of solar envelopes illustrated in Fig. 1, Osman Ural in TU Delft urbanism editing team for proofreading the preliminary manuscript, and TU Delft Library for supporting logistics and open access of this journal publication.

Appendix A. Supplementary data

Supplementary data to this article can be found online at https://doi.org/10.1016/j.rser.2020.109742.

References

[1] van Hove L, Steeneveld G, Jacobs C, Heusinkveld B, Elbers J, Moors E, Holtslag A. Exploring the urban heat island intensity of Dutch cities. Wageningen: Wageningen University and Alterra Report 2170; 2011.
[2] Nations U. United Nations framework convention on climate change. 1992. United Nations, Rio de Janeiro.
[3] Wainwright O. The Walkie-Talkie skyscraper, and the City's burning passion for glass. The Guardian; 3 September 2013 [Online]. Available: https://www.theguardian.com/commentisfree/2013/sep/03/walkie-talkie-skyscraper. [Accessed 7 July 2019].
[4] Knowles RL. Energy and form: an ecological approach to urban growth. Cambridge: The MIT Press; 1974.
[5] Knowles RL. Sun, rhytm and form. Massachusetts: The MIT Press; 1981.
[6] Alkadri MF, Turrin M, Sariyildiz S. The use and potential applications of point clouds in simulation of solar radiation for solar access in urban contexts. Adv Comput Des 2018;3(4):319–38.
[7] Stasinopoulos TN. A survey of solar envelope properties using solid modelling. J Green Build 2018;13(1):3–30.
[8] De Luca F, Dogan T. A novel solar envelope method based on solar ordinances for urban planning. Build Simulat 2019;12(5):817–34.
[9] De Luca F. Solar form finding. Subtractive solar envelope and integrated solar collection computational method for high-rise buildings in urban environments. In: Proceedings of disciplines and disruption 37th annual conference of the association for computer aided design in architecture. Cambridge, United States: ACADIA; 2017. p. 212–21.
[10] Arayici Y, Hamilton A, Gamito P. Modelling 3D scanned data to visualize and analyse the built environment for regeneration. Survey Built Environ 2006;17(2):7–28.
[11] Arayici Y. Towards building information modelling for existing structures. Struct Surv 2008;26(3):210–22.
[12] Alkadri MF, Turrin M, Sariyildiz S. A computational workflow to analyse material properties and solar radiation of existing contexts from attribute information of point cloud data. Build Environ 2019;155:268–82.
[13] Stevenson D. A proposal for the irrigation of the hanging Gardens of Babylon. Iraq 1992;54:35–55.
[14] Wiseman DJ. Mesopotamian Gardens. Anatol Stud 1983;33:137–44.
[15] Mazzone D. The dark side of a model community: the 'ghetto' of el-lahun. J Ancient Egypt Architect 2017;2:19–54.
[16] Butti K, Perlin J. A golden threat 2500 Years of solar architecture and technology. Van Nostrand Reinhold Company; 1980. New York.
[17] Capeluto IG, Shaviv E. Modelling the design of urban fabric with solar rights considerations. In: International conference of IBPSA; 1997. Kyoto.
[18] Capeluto I, Yezioro A, Bleiberg T, Shaviv E. From computer odels to simple design tools: solar rights in the design of urban streets. In: Ninth international IBPSA conference; 2005. Montreal.
[19] Capeluto GI, Plotnikov B. A method for the generation of climate-based, context-dependent parametric solar envelopes. Architect Sci Rev 2017;60(5):395–407.

[20] Machacova K, Keppl J, Krajcovics L. The solar envelope method in education at the faculty of architecture STU Bratislava. In: Central Europe towards sustainable building; 2013. Prague.
[21] Martin CL, Keeffe G. The Biomimetic solar city: solar derived urban form using a forest-growth inspired methodology. In: The 24th Conference on passive and low energy architecture; 2007. Singapore.
[22] Martin CL, Pilling M, Stott C, Walsh V. The nectar project: solar development of post-industrial urban communities. In: The 27th conference on passive and low energy architecture. Louvain-la-Neuve; 2011.
[23] Dekay M. The implications of community gardening for land use and density. J Architect Plann Res 1997;14(2):126–49.
[24] De Luca F. Solar envelope optimization method for complex urban environments. In: CAADence in architecture; 2016. Budapest.
[25] Bruce G. High density, Low energy: achieving useful solar access for Dublin's multi-storey apartment developments. In: PLEA; 2008. Dublin.
[26] Saleh MM, Al-hagla KS. Parametric urban comfort envelope: an approach toward a responsive sustainable urban morphology. Int J Civil, Environ, Struct, Construct Architect Eng 2012;6(11):930–7.
[27] Noble D, Kensek K. Computer generated solar envelopes in architecture. J Architect 1998;3(2):117–27.
[28] Camporeale P. Genetic algorthims applied to urban growth optimization. In: eCAADe conference; 2013. Delft.
[29] Littlefair PJ, Santamouris M, Alvarez S, Dupagne A, Hall D. Environmental site layout planning: solar access, microclimate and passive colling in urban areas. Construction research communications Ltd; 2000. London.
[30] Capeluto IG, Yezioro A, Bleiberg T, Shaviv E. Solar rights in the design of urban spaces. In: The 23rd conference on passive and low energy architecture; 2006. Geneva.
[31] Brandao RS, Alucci MP. Solar access in tropical cities: towards a multicriteria solr envelope. In: The 22nd Conference on passive and low energy architecture; 2005. Beirut.
[32] Pereira FOR, Silva CAN, Turkienikz B. A methodology for sunlight urban planning: a computer based solar and sky vault obstruction analysis. Sol Energy 2001;70(3):217–26.
[33] Grazziotin PC, Pereira FOR, Freitas CMDS, Turkienicz B. Integration of sunlight access control to building potential simulator. In: The ibero-American symposium on computer graphics; 2002. Guimaraes.
[34] Turkienicz B, Goncalves BB, Grazziotin P. CityZoom:A Visualization Tool for the assessment of plannning regulations. Int J Architect Comput 2008;6(1):79–95.
[35] Amaral MDGVD. The application of solar architecture in the planning of the campus. In: The 2005 World sustainable building cocnfrenec; 2005. Tokyo.
[36] Paramita B, Koerniawan M. Solar envelope assessment in tropical region building case study: vertical settlement in Bandung, Indonesia. In: The 3rd International conference on sustainable future for human security SUSTAIN. vol. 2012; 2013. Kyoto.
[37] Emmanuel R. A hypothetical 'shadow umbrella' for thermal comfort enhancement in the equatorial urban outdoors. Architect Sci Rev 1993;36(4): 173–84.
[38] Lobaccaro G, Frontini F, Masera G, Poli T, SolarPW ". A new solar design tool to exploit solar potential in existing urban areas. Energy Procedia 2012;30:1173–83.
[39] Dekay R. Climatic urban design: configuring the urban fabric to support daylighting, passive cooling, and solar heating. Sustain city VII 2012;155:619–30.
[40] DeKay M. Daylighting and urban form: an urban fabric of light. J Architect Plann Res 2010;27(1):35–56.
[41] Okeil A. A holistic approach to energy efficient building forms. Energy Build 2010;42(9):1437–44.
[42] Okeil A. In search for energy efficient urban forms: the residential solar block. In: "BUilding for the future: the 16th CIB world building congress 2004; 2004. Rotterdam.
[43] Raboudi K, Saci AB. A morphological generator of urban rules of solar control. In: The 29th conference Sustainable architecture for a renewable future; 2013. Munich.
[44] Stasinopoulos TN. "Solar envelope - a construction method using AutoCAD 2000," 9. July 2001 [Online]. Available: http://www.oikotekton.eu/solenvelope. [Accessed 25 October 2016].
[45] Kensek K, Henkhaus A. Solar access zoning + building information modeling. In: Solar 2013; 2013. Baltimore.
[46] Vartholomaios A. The residential solar block envelope: a method for enabling the development of compact urban blocks with high passive solar potential. Energy Build 2015;99:303–12.
[47] Cotton JF. Solid modeling as a tool for constructing solar envelopes. Autom ConStruct 1996;5(3):185–92.
[48] Niemasz J, Sargent J, Reinhart CF. Solar zoning and energy in detached dwellings. In: SimAUD; 2011. Boston.
[49] Morello E, Ratti C. Sunscapes: ''solar envelopes' and the analysis of urban DEMs. Comput Environ Urban Syst 2009;33(1):26–34.
[50] Ratti C, Morello E. Sunscapes: extending the 'solar envelopes' concept through 'iso-solar surfaces. In: The 22nd conference on passive and low energy architecture; 2005. Beirut.
[51] Maas W. What's next?: how do we make vertical urban design?. In: Council on tall buildings and urban habitat (CTBUH); 2016. Shenzen.
[52] White DA. LIDAR, point clouds, and their archaeological applications. In: Mapping archaeological landscapes from space. Springer-Verlag New York; 2013. p. 175–86. New York.
[53] Otepka J, Ghuffar S, Waldhauser C, Hochreiter R, Pfeifer N. Georeferenced point clouds: a survey of features and point cloud management. ISPRS Int J Geo-Inf 2013;2(4). 2038-1065.
[54] Weinmann M. Reconstruction and analysis of 3D scenes. Springer International Publishing; 2016. Karlsruhe.
[55] Randall T. Client guide to 3D scanning and data capture. BIM Task Group; 2013. UK.
[56] Kobayashi I, Fujita Y, Sugihara H, Yamamoto K. Attribute analysis of point cloud data with color information. J Japan Soc Civil Eng 2011;67(2):95–102.
[57] Fujita Y, Hoshino Y, Ogata S, Kobayashi I. Attribute assignment to point cloud data and its usage. Global J Comput Sci Technol 2015;15(2):2–B.
[58] Fujita Y, Kobayashi I, Hoshino Y, Chanseawrassamee W. Development of attribute-assign-editor for road surface point cloud data. IACSIT Int J Eng Technol 2016;8(3):170–6.
[59] Kaasalainen S, Krooks AKA, Kaartinen H. Radiometric calibration of terrestrial laser scanners with external reference targets. Rem Sens 2009;1(3):144–58.
[60] Kashani AG, Olsen MJ, Parrish C, Wilson N. Review of LIDAR radiometric processing: from ad hoc intensity correction to rigorous radiometric calibration. Sensors 2015;15(11):28099–128.
[61] Gressin A, Mallet C, Demantké J, David N. Towards 3D lidar point cloud registration improvement using optimal neighborhood knowledge. ISPRS J Photogrammetry Remote Sens 2013;79:240–51.
[62] Salehi V, Wang S. Using point cloud technology for process simulation in the context of digital factory based on a system engineering integrated approach. In: The 21st international conference on engineering design. ICED 17); 2017. Vancouver.
[63] Sidiropoulou-Velidou D, Georgopoulos A, Lerma JL. Exploitation of thermal imagery for the detection of pathologies in monuments. In: Progress in cultural heritage preservation. 4th International Conference; 2012. EuroMed 2012, Limassol.
[64] Gigliarelli E, Carlea D, Corcella A, Porfyriou H. Historical social housing: smart analysis and design for conservation and energy conservation. In: Progress in cultural heritage preservation. 4th International Conference; 2012. EuroMed 2012, Limassol.
[65] Staneva NN. Approaches for generating 3D solid models in AutoCAD and solid works. J Eng 2008;VI(3):28–31.
[66] Shapiro V. "Solid modeling," spatial automation laboratoty. Madison: University of Wisconsin; 2001.
[67] Richter R, Döllner J. Concepts and techniques for integration, analysis and visualization of massive 3D point clouds. Comput Environ Urban Syst 2014;45: 114–24.
[68] Mallet C. Analyse des données lidar aéroportées à Retour d'Onde Complète pour la cartographie des milieux urbains. Paris: De Télécom ParisTech; 2010.
[69] Bueno M, Martínez-Sánchez J, Gonzales H, Lorenzo H. Detection of geometric keypoints and its application to point cloud coarse registration. Int Arch Photogram Rem Sens Spatial Inf Sci 2016;XLI(B3):187–94.
[70] Hollaus M, Höfle B, Dorigo W, Pfeifer N, Bauerhansl C, Regner B. Tree species classification based on full-waveform airborne laser scanning data. In: Proceedings of the SILVILASER; 2009. Texas.
[71] Heinzel J, Koch B. Exploring full-waveform LiDAR parameters for tree species classification. Int J Appl Earth Obs Geoinf 2011;13(1):152–60.
[72] Neuenschwander AL, Magruder L, Tyler M. Landcover classification of small-footprint, full- waveform lidar data. J Appl Remote Sens 2009;3(1):1–13.
[73] Shih N-J. The application of A 3d scanner in the representation of building construction site. In: International association for automation and robotics in construction. IAARC); 2002. Madrid.
[74] Várady T, Martin RR, Cox J. "Reverse engineering of geometric models—an introduction. Comput Aided Des 1997;29(4):255–68.
[75] Fujita Y, Kobayashi I, Chanseawrassamee W, Hoshino F. Application of attributed road surface point cloud data in road maintenance. J Japan Soc Civil Eng, Ser. F3 (Civil Eng Inf) 2014;70(2):I_185–92.
[76] Lin E, Girot C. Point cloud components tools for the representation of large scale landscape architectural projects. In: Digital landscape architecture; 2014. Zurich.
[77] Lin E, Shaad K, Girot C. Developing river rehabilitation scenarios by integrating landscape and hydrodynamic modeling for the Ciliwung River in Jakarta, Indonesia. Sustain Cities Soc 2016;20:180–98.
[78] Kersten TP, Keller F, Saenger J, Schiewe J. Automated generation of an historic 4D city model of hamburg and its visualization with the GE engine. In: Progress in cultural heritage, 4th international conference; 2012. EuroMed 2012, Limassol.
[79] M. Balzani, C. Bughi, F. Ferrari, L. Rossato and A. Tursi, Alberti's box: the cultural multimedia project on the architectures of leon battista alberti," in Progress in cultural heritage preservation, 4th International Conference, EuroMed 2012, Limassol, 2012.
[80] Moussa W, Abdel-Wahab M, Frisch D. Automatic fusion of digital images and laser scanner data for heritage preservation. In: Progress in cultural heritage preservation. 4th International Conference; 2012. EuroMed 2012, Limassol.
[81] Bornaz L, Lingua A, Rinaudo F. Engineering and envirоonmental applications of laser scanner techniques. In: ISPRS commission III symposium " photogrammetric computer vision; 2002. Graz.
[82] Kassner R, Koppe W, Schüttenberg T, Bareth G. Analysis of the solar potential of roofs by using official lidar data. In: ISPRS congress beijing; 2008. Beijing.
[83] Carneiro C, Morello E, Desthieux G. Assessment of solar irradiance on the urban fabric for the production of renewable energy using LIDAR data and image processing techniques. In: Advances in GIScience; 2009. Hannover.
[84] Ochmann S, Vock R, Wessel R, Klein R. Automatic reconstruction of parametric building models from indoor point clouds. Comput Graph 2016;54:94–103.

[85] Voegtle T, Schwab IR, Landes T. "Influences of different materials on the measurements of a terrestrial laser scanner (tls)," *the International Archives of the Photogrammetry*. Rem Sens Spatial Inf Sci 2008;37(5):1061–6.
[86] ArcMap. What is lidar intensity data?. 2016 [Online]. Available: http://desktop.arcgis.com/en/arcmap/10.3/manage-data/las-dataset/what-is-intensity-data-.htm. [Accessed 7 December 2018].
[87] Aurgho J. High rise morphologies: architectural form FInding in a performance design search space of dense urban contexts. In: The 35th annual conference of the association for computer aided design in architecture; 2015. Cincinnati.
[88] Leidi M, Schlüter A. Volumetric insolation analysis. In: CleanTech for sustainable buildings - from nano to urban scale. CISBAT 2011); 2011. Lausanne.
[89] Ozel F. SolarPierce: a solar path-based generative system. In: Computation and performance - proceedings of the 31st eCAADe conference; 2013. Delft.
[90] Foged IW. Architectural thermal forms. In: Computation and performance – proceedings of the 31st eCAADe conference; 2013. Delft.
[91] Armstrong L, Gardner G, James C. Evolutionary solar architecture - generative solar design through soft forms and rigid logics. In: Parametricism Vs. Materialism: evolution of digital technologies for development [8th ASCAAD conference proceedings]; 2016. London.
[92] Marin P, Bignon J-C, Lequay H. Generative exploration of architectural envelope responding to solar passive qualities. In: Design and decision support systems in architecture and urban planning [DDSS 2008]; 2008. Eindhoven.
[93] Da Veiga J, La Roche P. A computer solar analysis tool for the design and manufacturing of complex architectural envelopes: EvSurf. In: Proceedings of the 6th iberoamerican congress of digital graphics [SIGraDi 2002]. Caracas; 2012.
[94] Yang X, Grobe L, Stephen W. Simulation of reflected daylight from building envelopes. In: Proceeding of BS2013: 13th conference of international building performance simulation association; 2013. Chambery.
[95] Girardeau-Montaut D. Cloud-compare [Online]. Available:. 2015. http://www.cloudcompare.org/doc/qCC/CloudCompare%20v2.6.1%20-%20User%20manual.pdf. [Accessed 5 February 2018].
[96] Roudsari MS, Michelle P. Ladybug: a parametric environmental plugin for grasshopper to help designers create an environmentally-conscious design. " Lyon; 2013.
[97] Charlton ME, Coveney SJ, McCarthy T. Issues in laser scanning. In: Laser scanning for the environmental sciences. West Sussex: Wiley-Blackwell; 2009. p. 35–48.
[98] Bartolo SD, Salvini R. Multitemporal terrestrial laser scanning for marble extraction assessment in an underground quarry of the apuan alps (Italy). Sensors 2019;19(3):1–10.
[99] Faro. Faro laser scanner user manual. Florida: " Faro Technologies Inc.; 2018.
[100] Suchocki C, Błaszczak-Bąk W. Down-sampling of point clouds for the technical diagnostics of buildings and structures. Geosciences 2019;9(2):1–14.
[101] Armesto-González J, Riveiro-Rodríguez B, González-Aguilera D, Rivas-Brea MT. Terrestrial laser scanning intensity data applied to damage detection for historical buildings. J Archaeol Sci 2010;37(12):3037–47.
[102] Soudarissanane SS. The geometry of terrestrial laser scanning, Delft. PhD-thesis Facul Civil Eng Geosci 2016. TU Delft.
[103] Sasidharan S. A normalization scheme for terrestrial LiDAR intensity data by range and incidence angle. Int J Emerg Technol Adv Eng 2016;6(5):322–8.
[104] Boulch A, Marlet R. Deep learning for robust normal estimation in unstructured point clouds. In: Eurographics symposium on geometry processing; 2016. Berlin.
[105] Shin J, Park H, Kim T. Characteristics of laser backscattering intensity to detect frozen and wet surfaces on roads. J Sens 2019;(1):1–9. 2019.
[106] Szokolay SV. Introduction to architectural science: : the basis of sustainable design. Oxford: Elsevier/Architectural Press; 2008.
[107] Majcen D. Predicting energy consumption and savings in the housing stock. Delft: PhD dissertation - ABE tudelft; 2016.
[108] Chwieduk D. Solar energy in buildings: thermal balance for efficient heating and cooling. London: Elsevier Science Publishing Co Inc; 2014.